



HAL
open science

Preliminary results of a paleoseismological analysis along the Sahel fault (Algeria): New evidence for historical seismic events

A. Heddar, Christine Authemayou, H. Djellit, K. Yelles, Jacques Déverchère, S. Gharbi, A. Boudiaf, Brigitte van Vliet-Lanoë

► To cite this version:

A. Heddar, Christine Authemayou, H. Djellit, K. Yelles, Jacques Déverchère, et al.. Preliminary results of a paleoseismological analysis along the Sahel fault (Algeria): New evidence for historical seismic events. *Quaternary International*, 2013, 302, pp.210-223. 10.1016/j.quaint.2012.09.007 . insu-00841173

HAL Id: insu-00841173

<https://insu.hal.science/insu-00841173>

Submitted on 9 Jul 2013

HAL is a multi-disciplinary open access archive for the deposit and dissemination of scientific research documents, whether they are published or not. The documents may come from teaching and research institutions in France or abroad, or from public or private research centers.

L'archive ouverte pluridisciplinaire **HAL**, est destinée au dépôt et à la diffusion de documents scientifiques de niveau recherche, publiés ou non, émanant des établissements d'enseignement et de recherche français ou étrangers, des laboratoires publics ou privés.

1 **Preliminary results of a paleoseismological analysis along the Sahel fault (Algeria):**
2 **new evidence for historical seismic events**

3
4 *Heddar, A^a, Authemayou, C^b, Djellit, H.^A, Yelles, A.K^a,*
5 *Deverchere, J.^B, Gharbi, S^a, Boudiaf, A.^C, Van Vliet Lanoe, B^b*

6
7 ^a CRAAG Centre de Recherche en Astronomie Astrophysique et Géophysique, - Route de
8 l'Observatoire Bp 63 Bouzareah - Alger – Algeria

9 ^b Université de Brest (UBO), UMR 6538 Domaines Océaniques, 29238 Plouzané, France

10 ^c Université de Montpellier, France

11
12 *Abstract*

13 The ~60 km-long Sahel ridge west of Algiers (Tell Atlas, north Algeria) is considered as an
14 ENE-WSW fault-propagation fold running along the Mediterranean coast and associated with
15 a north-west dipping thrust. Its proximity with Algiers makes this structure a potential source
16 of destructive earthquakes that could hit the capital city, as occurred in 1365 AD and 1716
17 AD. The first paleoseismologic investigation on the Sahel ridge was conducted in order to
18 detect paleo-ruptures related to active faulting and to date them. From the first investigations
19 in the area, a first trench was excavated across bending-moment normal faults induced by
20 flexural slip folding in the hanging wall of the Sahel anticline thrust ramp. Paleoseismological
21 analyses recognize eight rupture events affecting colluvial deposits. ¹⁴C dating indicates that
22 these events are very young, six of them being younger than 778 AD. The first sedimentary
23 record indicates two ruptures before 1211 AD, i.e. older than the first historical earthquake
24 documented in the region. Three events have age ranges compatible with the 1365, 1673 and
25 1716 Algiers earthquakes, whereas three other ones depict very recent ages, i. e. younger than
26 1700 AD. Potential of these secondary extrados faults for determining paleoseismic events
27 and thrust behaviour is discussed.

28 **Keywords:** *Algeria, Sahel, paleoseismology, trench, rupture event, historical earthquake*

29
30 **1. Introduction**

31 North Algeria was affected by several large ($M > 7$) earthquakes in recent centuries
32 (Meghraoui et al., 1988; Bezzeghoud et al., 1996). Although strain rates are low compared to
33 those occurring along subduction zones, their impacts on human lives and infrastructures
34 appear to be quite high in the light of this historical knowledge. One of the most seismically

35 active areas in Algeria is the part of the Tell Atlas located in Northernmost Algeria (Fig. 1).
36 Many catalogs of seismicity have reported moderate and shallow seismicity punctuated by
37 strong earthquakes (Rothé, 1950; Hée, 1950; Roussel, 1973; Benhallou, 1985; Mokrane et al.,
38 1994; Benouar, 1994; Yelles et al., 2002; Harbi et al., 2004, 2007a). In recent decades, this
39 area has experienced destructive earthquakes, such as Orléansville on 09/09/1954 ($M=6.7$)
40 (Rothé, 1955), El Asnam on 10/10/1980 ($M=7.3$) (Ouyed et al., 1980), Tipaza on 29/10/1989
41 ($M=6.0$) (Meghraoui, 1991), and Boumerdes-Zemmouri on 21/05/2003 ($M=6.8$) (Ayadi et
42 al., 2003), making this territory one of the most seismic regions in the western Mediterranean.
43 It is a strategic area because of the location of the capital, Algiers, and other major cities,
44 where population and main social and economic activities are concentrated. Geodynamically,
45 the Tell Atlas corresponds to the passive margin of the Algerian back-arc basin, produced by
46 the roll-back of the Tethyan oceanic slab ending with the Miocene collision of the Kabyle
47 blocks with the African plate (Carminati et al. 1998; Gueguen et al., 1998; Vergès and Sabàt,
48 1999; Frizon de Lamotte, 2000; Jolivet and Faccenna, 2000; Mauffret et al., 2004; Duggen et
49 al., 2004; Schettino and Turco, 2006). Currently, the convergence between Africa and Eurasia
50 reactivates this margin in compression (Thomas, 1976; Domzig, 2006, Domzig et al., 2006,
51 Serpelloni et al., 2007). Analyses of focal mechanisms, GPS, VLBI (Very Long Baseline
52 Interferometry) and SLR (Satellite Laser Ranging) data indicate a NW-SE shortening
53 direction with a convergence rate of about 4-6 mm /y (Anderson and Jackson, 1987; De Mets
54 et al., 1990; Stich et al., 2006; Serpelloni et al., 2007).

55 This shortening affects faulted and folded structures in the onshore and offshore domains
56 (Thomas, 1976; Philip and Meghraoui, 1983; Domzig, 2006; Domzig et al., 2006; Yelles et
57 al., 2006). Some of these structures are inherited and experienced thrust and/or strike-slip
58 faulting. The most well-known structure in Algeria is the Oued Fodda (El Asnam) NE-SW
59 sinistral reverse fault associated with an anticlinal ramp that generated the strongest
60 earthquake in the western Mediterranean on October 10, 1980 ($M_s: 7.3$) (Ouyed et al., 1981,
61 1982; King and Vita-Finzi, 1981; Yielding et al., 1981; Deschamps et al., 1982) (Fig. 1). The
62 first paleoseismological investigation realized in Algeria was made on this fault. It recognized
63 the existence of clusters of large earthquakes alternating with periods of quiescence, and a
64 return period between 300 and 400 years during the active faulting episodes (Meghraoui and
65 al., 1988). Close to Algiers, the Mitidja basin is bounded by several major active structures,
66 which are the sources of potential destructive earthquakes (Meghraoui, 1991; Boudiaf, 1996;
67 Harbi et al., 2004; Guemache et al., 2010; Maouche et al., 2011) (Fig. 1). In the instrumental
68 period, moderate earthquakes ($M<6$) have been recorded with no surface ruptures (Oued Djer

69 event (M 5.5) in 1988; Tipaza event (M 6.0) in 1990; Ain-Benian event (M 5.7) in 1996
70 (Bezzeghoud et al., 1996; Boudiaf, 1996; Mokrane et al., 1994; Sebaï, 1997). The Mw 6.8
71 Boumerdes (05/21/2003) earthquake was accompanied by substantial coastal uplift but did
72 not produce observable surface ruptures, probably because it was located offshore
73 (Déverchère et al., 2005, 2010). Nevertheless, the Algiers region has experienced in the
74 historical period damaging earthquakes (e.g., 1365, 1716), (Ambraseys and Vogt, 1988; Harbi
75 and al, 2007a) that have not until now been attributed definitely to a specific structure of the
76 Mitidja basin or surrounding faults.

77 This paleoseismological study deals with an active structure located north of the Mitidja
78 basin. It focuses on the north-west dipping reverse fault of the Sahel anticline emerging near
79 the Mediterranean shoreline (Figs. 1 and 2). The purpose of this study is to detect surface
80 ruptures that record paleo-earthquakes in an attempt to complement the seismologic catalog of
81 the region and give the first direct evidence of surface ruptures produced by the Sahel
82 structure activity. The investigated site has been selected after analyses of SPOT satellite
83 imagery and field investigations. It is located on the southern flank of the Sahel fault
84 propagation fold, in the region of Kolea city, across extrado-type normal faults affecting
85 recent colluvial deposits (Fig. 2). These flexural faults are associated with the major reverse
86 thrust activity located in the piedmont plain. Until now, no studies have detected the surface
87 breaks of this thrust that appears as a blind structure under the thick Quaternary alluvial
88 deposits of the Mitidja basin. However, paleoseismologic analyses of the secondary normal
89 faults allow reporting for the first time historical seismic ruptures associated with the activity
90 of the Sahel structure. As underlined by McCalpin (2009), the results also show that
91 paleoseismic history derived from secondary faults may be a good proxy for events on the
92 underlying thrust, especially where this latter does not extend to the surface. Secondary faults
93 in the study area form a graben corresponding to a sediment trap with abundant organics for
94 ^{14}C dating.

95

96 **2. Seismotectonic framework**

97 *2.1 Geological setting*

98 The E-W Mitidja plain is a Middle Miocene to Quaternary intra-continental basin (Figs. 1 and
99 2) (Glangeaud et al., 1952; Aymé et al., 1954). Its sedimentary filling consists of Miocene to
100 Pliocene marine marls, calcareous and sandstones covered by Quaternary heterogeneous
101 continental deposits that have been subsequently partially eroded (Glangeaud, 1932). The
102 basin was interpreted variously as a graben (De Lamothe, 1911) or a syncline bounded by

103 compressive structures (Glangeaud, 1932). The lack of seismic profiles and deep wells across
104 the basin prevents knowing its depth, precise timing of development, geometry and dip of the
105 surrounding faults. Only the modeling of recent gravity data has highlighted a deep and steep
106 north-dipping tectonic contact oriented NE-SW at the northern basin boundary (Hamaï,
107 2011).

108 The Mitidja basin is surrounded by relief belonging to different structural domains, namely
109 the Atlas of Blida Mountains to the south and the Chenoua-Sahel-Bouzareah relief to the
110 north (Fig. 1). To the south, the Atlas of Blida Mountains reaches 1500 m height. This relief
111 consists mainly of Tellian units composed of flysch and Cretaceous deposits (Blès, 1971).
112 The northern boundary of the Blida Atlas Mountains shows Pliocene deposits dipping to the
113 north affected by a reverse fault (Glangeaud et al., 1952; Bonneton, 1977; Boudiaf, 1996;
114 Guemache, 2010; Guemache et al., 2010). This reverse fault extends to the east, close to the
115 coastline (Meghraoui et al., 2004; Ayadi et al., 2008). Boudiaf (1996) has recognized
116 Quaternary activity on this structure.

117 To the north, the Mitidja basin is separated from the Mediterranean Sea by the Chenoua and
118 Algiers-Bouzareah massifs which are relics belonging to the Internal Zones (Durant-Delga,
119 1969) formed by discontinuous massifs spread along the coast. The Bouzareah massif is made
120 of a metamorphic block (Saadallah, 1981), whereas the Chenoua massif comprises a
121 sedimentary sequence from the Devonian to the Oligocene (Belhai, 1987, Belhai et al., 1990)
122 (Fig. 2). The latter massif is bounded to the south by a 10 km-long EW-trending reverse fault
123 bent northeastward in the offshore domain (Meghraoui, 1991).

124 Between the two massifs, the 60 km-long WSW-ENE Sahel ridge runs along the coast. It is
125 formed by hills of moderate altitude (~200 m) and tablelands, and shows a morphological
126 discontinuity formed by the across-strike valley of the Mazafran River (Fig. 2). The Sahel
127 structure is generally interpreted in two ways. Aymé et al. (1954) proposed that the ridge
128 corresponds to a monoclinical series of Neogene deposits formed of Miocene and Pliocene
129 marls and sandstones (Fig. 2, cross-section B). More recently, several authors (Meghraoui,
130 1988, 1991; Maouche et al., 2011) interpreted this structure as a south-verging asymmetric
131 fault-propagation fold formed by Pliocene units overlapped by marine terrace deposits
132 (Aymé, 1952; Saoudi, 1989) that was developed in response to the motion on a 60 km-long
133 north-west dipping blind thrust fault, south of the ridge, which they refer to as the Sahel fault
134 (Fig. 2, cross-section A). Offshore, two other 20 km-long NE-trending reverse faults have
135 been detected affecting the upper Khayr-al-Din bank (Yelles et al., 2009; Fig. 2).

136 This study focuses on the largest structure of the northern boundary of the Mitidja basin, the
137 Sahel ridge, which represents a young tectonic feature formed after the Pliocene. To compare
138 the two interpretations of an onshore anticline (Megrahoui, 1991) or onshore monocline
139 (Aymé, 1954), it is proposed that the Sahel ridge is an anticline potentially extending
140 offshore. This discrepancy is secondary for the purpose of this study, as the aim is to establish
141 paleoseismological analyses across secondary faults associated with the blind thrust on the
142 southern Sahel flank.

143

144 2.2 *Historical and instrumental seismicity*

145 Many studies producing catalogs on historical seismicity report several earthquakes that have
146 struck Algiers and its surroundings, but their locations remain uncertain or controversial
147 (Rothé, 1950; Benhallou et al., 1971; Roussel, 1973; Ambraseys and Vogt, 1988; Mokrane et
148 al., 1994; Benouar, 1994; Harbi, 2006; Harbi et al., 2004, 2007a; Sebaï and Bernard 2008;
149 Fig. 1). Among the most cited events, a major earthquake occurred on January 3, 1365,
150 striking Algiers, inducing a tsunami, followed by about 500 aftershocks (Harbi et al., 2007a).
151 This damaging earthquake was located either offshore or near the coast, with an intensity (*I*)
152 of X on the EMS scale. Another event on February 3, 1716, much more documented (Perrey,
153 1847; Mokrane et al., 1994; Rothé, 1950; Benhallou et al., 1971; Roussel, 1973; Ambraseys
154 and Vogt, 1988; Harbi et al., 2004; 2006; 2007a), destroyed a large part of Algiers and Blida
155 (a city located 30 km to the south of Algiers). It caused the loss of 20,000 lives. Harbi et al.
156 (2007a) located its epicenter close to Douera in the Algiers Sahel, and Sebaï and Bernard
157 (2008) located it close to Algiers. Other historical earthquakes of intensity VIII have affected
158 the region near Algiers in 1673 and 1842 (Harbi et al., 2007a). Some other larger historical
159 earthquakes are documented, but their location or intensity are doubtful (in 1522 north of
160 Tipaza, located at the western part of the Sahel structure (*I*: IX); in 1658 around the Chenoua
161 Massif, in 1804 around Sidi Fredj, located at the coastline of the Algiers massif (*I*: IX) and in
162 1860 north of Tipaza (*I*: VIII).

163 Seismic monitoring began in Algeria after the 1980 El-Asnam earthquake (M 7.3). However,
164 the record has been continuous only since the establishment of the digital network in 2005.
165 This explains the lack of microseismicity recording necessary in order to identify and monitor
166 active structures. A moderate to low seismicity seems to be clustered near Algiers. Some
167 small events are located westward of the valley of Mazafran River (Fig.1 and 2). Recently,
168 two events occurred on 20-05-2010 (M 4.2) and on 23-11-2011 (M 3.4) that have been felt by
169 the population in the region of Algiers. They were located 4 km SW of Douera for the first

170 one and 4 km SE of Douera for the second (Centre de Recherche en Astronomie,
171 Astrophysique et Géophysique (CRAAG), 2010; 2011) (Fig. 1). Instrumental seismicity has
172 allowed identification of some active zones and focal mechanisms (Fig. 1). The most
173 important events are : Chenoua (M: 6.0) on 29/10/1989; Ain El Benian (M: 5.7), on
174 04/09/1996; and Boumerdes (Mw:6.8), on 21/05/2003 (Meghraoui, 1991; Maouche et al.,
175 1998; Bounif et al., 2003; Harbi et al., 2004, 2007b; Déverchère et al., 2005; Yelles et al.,
176 2004, 2006). These events are related to offshore faults close to the coast and are
177 characterized by reverse focal mechanisms (Fig. 1). Despite the substantial seismicity in the
178 Sahel region, no clear evidence of surface break after an earthquake was found.

179

180 **3. Paleoseismicity study**

181 *3.1. Trench location*

182 Satellite images analyses, gravimetry data (Hamai, 2011) and field investigations were used to
183 select a site in the south area of Kolea city, located 40 km SW of Algiers, on the southern
184 flank of the Sahel fold (Fig. 2). The first witnesses of active faulting near the surface were
185 highlighted by an abrupt change of the dip of the Astian upper layers from 31° to 84° toward
186 the SSE (sites 1 and 2, Figs. 2 and 3). This sharp flexure could have been produced by short
187 wave-length folding associated with motion along the major thrust.

188 Near these sites, visible on a SPOT 5 satellite image, is a morphological scarp 5 m high,
189 suspected as the fault trace of the major Sahel thrust (Fig. 4a). A paleoseismological analysis
190 of this scarp did not reveal fault ruptures but only gentle horizontal alluvial sediments and
191 marls above them (see Appendix). The scarp was formed by differential erosion of the upper
192 marl with respect to the conglomerates induced by incision of the surrounding Mazafran
193 River. Thus, it is suspected that the Sahel thrust would be masked by thick alluvial deposits.
194 However, 200-m upward from the scarp (Fig. 4b), in the slope of the southern flank of the
195 Sahel ridge, trench metric-scale normal faults affecting partially masked surface deposits are
196 exposed in earthworks. Farm activity has removed their geomorphologic expression at the
197 surface: however, cleaning revealed a local graben structure 5 m-long and 1.5 m-deep
198 affecting pedogenic marls filled by various ruptured colluvial deposits rich in charcoal (Fig.
199 5). After the enlargement of the earthwork trench in May 2012, a major 20-m high normal
200 fault dipping to the north was observed 8 m southward, affecting Pliocene sandstones and
201 forming a half-graben filled by Quaternary conglomerate deposits. This Quaternary infilling
202 extended deeper into the fault plane, forming a fissure fill facies suggesting piping process or
203 a fissure-graben model in a context of a humid period during the earthquake (Fig. 6) (Higgins

204 and Coates, 1990; McCalpin, 2009). These extensional structures are commonly observed in
205 anticlinal ramp systems, named extradors faults or moment-bending faults: they are produced
206 by flexural slip folding during motion along the anticlinal ramp (Fig. 4b). These kinds of
207 structures have been observed and described in Iran on the hanging wall of the Tabas thrust
208 during the 1978 Tabas-e-Goldshan earthquake (Berberian, 1979), in Algeria on the Oued
209 Fodda fault-propagation fold during the 1980 El-Asnam damaging earthquake (Philip and
210 Meghraoui, 1983), south of the Chenoua Massif during the 1989 Mont Chenoua-Tipaza
211 earthquake (Meghraoui, 1991), and on the Sahel structure (Maouche et al., 2011). Faults
212 encountered on this latter site must have the same tectonic origin, especially as the gentle dip
213 of the slope of 6-7° to the south and the dip of the normal faults opposite to this slope prevent
214 interpreting them as effects of gravity motion.

215 During spring 2011, a paleoseismological study focused on the normal faults of the graben,
216 because even if these secondary faults are not large enough to be seismogenic, paleoseismic
217 histories derived from them may be good proxies for events on the underlying seismogenic
218 thrust, especially where this one does not extend to the surface (McCalpin, 2009). The interest
219 in this structure relies is that the graben is a sediment trap with an important number of units
220 rich in organics for ¹⁴C dating, affected by several normal faults that allow recording a non-
221 negligible number of paleo-events. After having established an arbitrary system grid, the
222 trench was logged in detail, allowing a precise description of the deposits and paleosurface
223 ruptures.

224

225 *3.2. Stratigraphic Sequences*

226 The wall of the trench exhibits an elongated depression controlled by faulting as a graben
227 structure and filled by a well-defined sequence of tens of sub-horizontal colluvial deposits
228 (Fig. 5). The faults affect thick units of ochre white-spotted pedogenic marls corresponding to
229 alteration clay (unit 2) in contact to the south with tilted alluvial deposits (Unit 1). The
230 younger colluvial deposits (U3 to U12) were trapped in the graben, interpreted to be produced
231 by flexure in the hanging-wall of the anticlinal ramp thrust during successive seismic events.

232 The non-erosive flat boundaries between Units 3 to 10 indicate that most of the layers were
233 deposited without significant erosion of the underlying unit before deposition on a gentle
234 dipping slope. However, fragments of marls, more or less numerous from unit to unit, indicate
235 that the substratum of marls was eroded to feed in part the colluvial deposits as a scarp-
236 derived colluvium (McCalpin, 2009). These deposits have various colors, thicknesses and
237 extents and contain charcoal and shells (Fig. 5). Two different groups of units were

238 distinguished according to their lithologic contents. The limit between them is located at 1.10
239 m below the surface. The lower group is made of ochre detrital units (U3 to U5) with a
240 maximum total thickness of 22 cm. These colluvial deposits are mainly composed of
241 millimetre to centimetre gravels in a silty clay matrix.

242 The upper group (U6 to U12) includes units of brown to light clay, including a peat horizon.
243 These layers are essentially composed of silty clay containing shells and detrital charcoal.
244 Their colors vary from dark brown to yellow according to their abundance of organic matter.
245 A dark and thin peat horizon ~5 cm-thick (U8) is interstratified in the middle of the sequence
246 (Fig. 5). Unit 12 is unconformable above the older units, indicating a dominant erosional
247 control on its deposition. Unit 12 is rich in pedogenic marls provided by the denudation of the
248 marl substratum (U2). Finally, a brown surface layer of ~40 cm thick containing some detrital
249 charcoal seals the graben (U13) (Fig. 5).

250 According to the unit characteristics, the infill of the depression is related to sheet wash
251 erosion by local heavy precipitation as also shown laterally by piping at the level of the fault
252 (Fig. 6) (Higgins and Coates, 1990). Because of the location and orientation of the graben in
253 the general slope of the southern limb of the Sahel ridge and normal to the slope dip,
254 sedimentation is more related to colluvial activity than to fluvial influx, as indicated by the
255 shortage of gravels and lack of erosive discontinuities. The sequence corresponds to a step by
256 step infill of a depression with temporary stabilization allowing organic matter accumulation
257 (Unit 8).

258

259 3.3. Age control

260 In order to date the ruptures observed in the trench, we have sampled eleven detrital wood
261 fragments and gastropod shells in all units, except U3 and U5 which do not contain any
262 organic matter for ^{14}C dating (Fig. 5, Table 1). Gastropod shells correspond to *Helix aspera* in
263 Unit 4 (e1) and Unit 7 (e3). Caution in extracting samples has been taken to avoid
264 contamination. Samples were prepared for ^{14}C accelerated mass spectrometry (AMS) and
265 dated at the Poznan radiocarbon laboratory in Poland and at the Center for Applied Isotope
266 Studies University of Georgia (CAIS) in USA (Table 1). The ^{14}C ages were corrected for
267 changes in the atmospheric $^{14}\text{C}/^{13}\text{C}$ ratio over the last few millennia using IntCal, an on-line
268 CALIB Manual 6.0 radiocarbon calibration tool hosted by the Quaternary Isotope Laboratory
269 at the University of Washington, UK (<http://calib.qub.ac.uk>). For more accuracy, dates of
270 samples with a weight inferior to 0.2 mgC were not considered, because they were indicated
271 as unreliable by the Poznan radiocarbon laboratory (e2, e4, e9, Table 1). Furthermore,

272 samples with calibrated ages younger than 1750-1800 A.D. were described as "modern"
273 because they are located on the "plateau" of calibration and cannot be easily calibrated (e7,
274 e8, e9, e11, Table 1).

275 Samples of Units 4, 7, 8 have radiocarbon calibrated age ranges of 778-897 A.D., 1171-1211
276 A.D. and 1727-1779 A.D., respectively (Table 1, Fig. 5). The samples extracted in the middle
277 of Unit 9 and in the boundary of Units 9 and 10 are dated at 1304-1365 A.D. and as
278 "modern", respectively. The sample of the base of U12 provides a calibrated radiocarbon age
279 of 1455-1654 A.D. Samples of Units 10 and 13 are "modern".

280 Six of the eight ages are in stratigraphic order (Fig. 5). They correspond to samples collected
281 in Units 4, 7, 8; at the boundary between Units 9 and 10; in Unit 10; and Unit 13. The samples
282 of Units 9 and 12 give ages older than the age of the underlying unit. These anomalies suggest
283 that the samples have been reworked and redeposited several times. Sample dates in
284 stratigraphic order suggest rapid colluvial reworking and sedimentation, whereas the other
285 ones suggest multiphase reworking before sedimentation, which explains why younger dates
286 are below the dated unit. Furthermore, reworking is also suggested by weathered sampled
287 gastropods not observed in life position. With the process of reworking, all samples are older
288 than colluvial deposits, and thus give only a maximum age for each unit. Samples with older
289 dates than underlying samples (e6, e10) are useless because a better maximum age is given by
290 the dated underlying unit. Therefore, they will not be taken into account for the
291 paleoseismological interpretations.

292 Consequently, as Unit 4 has a sample date of 778-897 A.D. and is younger than Unit 7
293 associated with a sample dated at 1171-1211 A.D., Unit 4 is younger than 778 A.D. and older
294 than 1211 A.D. Concerning Unit 7, it contains a sample dated at 1171-1211 A.D., and the unit
295 is older than Unit 8, including a sample dated at 1727-1779 A.D. Thus, Unit 7 is younger than
296 1171 A.D. and older than 1779 A.D. Unit 8 has a sample age of 1727-1779 A.D.:
297 consequently, this unit is younger than 1727 A.D.

298 A minimum age could be attributed to Unit 8 and the above units containing "modern"
299 samples because the presence of a thick surface brown unit (U13) on top of these units
300 strongly suggests that it was formed after the agricultural reform in 1963 A.D. (Bessaoud,
301 1980). Thus, units designated "modern" have a range of ages between 1750 and 1963 AD
302 (Reimer et al., 2009).

303

304 *3.4. Evidence for faulting*

305 Considering the position of the outcrops relative to the blind, active thrust of the Sahel
306 anticline (Fig. 4b), offsets along normal faults observed in the trench are interpreted as effects
307 of flexure with extrados deformation related to the incremental growth of an anticline ramp in
308 the hanging wall of the blind thrust, produced during earthquakes in a way similar to what has
309 been reported in El Asnam site (Philip and Meghraoui, 1983; Meghraoui et al., 1988).
310 Analyzes of these extensional structures are critical to distinguish surface ruptures during
311 major paleo-earthquakes when the major thrust is blind (McCalpin, 2009).

312 A piece of evidence that the sediment trap in pedogenic marls corresponds to a graben is the
313 staircase geometry of its boundaries. Steep walls cannot be formed by erosion of marls;
314 because they would be smoother with gentle slopes. Each step must be bounded by a normal
315 fault, such as the surrounding normal fault located 8-m southward (Fig. 6). Furthermore, the
316 location of the sediment trap in the general slope of the southern limb of the Sahel anticline
317 and normal to the slope dip preclude characterizing it as a small erosional valley (Fig. 4b).

318 Different structural and sedimentological markers in the trench allow recognition of eight
319 rupture events associated with normal faulting. These markers correspond to sub-vertical
320 offsets of units along faults, and commonly folding of units on top of a fault termination,
321 because the clay-rich sediments result in plastic accommodation of the deformation. Drag
322 folds were observed close to the fault; shear zone or steep fault scarps bounded by units
323 representing colluvial wedges (Figs. 5a, b). Generally for the latter case, immediately after
324 faulting, the space produced by motion along a normal fault affecting a sloping surface is
325 filled by colluvial deposits mainly near the free face due to the continuous slope erosion by
326 streaming (McCalpin, 2009). The final geometry of the colluvial unit is generally asymmetric
327 with a maximum thickness at the fault plane. If two antithetic normal faults have the same
328 amount of motion during one event, the colluvial deposit shape is roughly symmetric. The
329 thickness of the colluvial unit corresponds to the minimum offset along the fault for one event
330 because the deposit and the fault scarp can be partially eroded.

331 In the trench, the 5m-long depression striking NW-SE exhibits five normal steep antithetic
332 metric-scale faults labeled A, B, C, D, and E (Fig. 5). Two (A and B), situated downward, dip
333 to the north, and the three others (C, D and E) dip to the south. They affect Units 3 to 12
334 differently.

335 Fault A constitutes the edge of Units 4, 5, 6, 8, 9, 10 and 12, with a thickening of Units 4, 5
336 and 6 near the fault (Fig. 5). The fault plane corresponds to a steep wall of marls and a shear
337 zone downward in the marls (Fig. 5a). Units 4, 5, 8 and 10 exhibit drag folds, indicating that
338 motion along the fault has affected these units. Fault B forms a fault plane that becomes

339 divided into two branches from Unit 6. It bounds Units 3 and 7, indicating that its motion has
340 controlled their deposition during two successive events. This motion has also shifted the base
341 of Units 5, 6 and 8 with a cumulative offset of 30 cm for Unit 5 and 6 and 17 cm for Unit 8
342 (Fig. 5). Finally, the northern branch of the fault activity has flexured Units 9 and 10 of 11 cm
343 and 8 cm, respectively. Fault C forms the northern edge of Units 3, 4, 5. Fault D bounds Unit
344 7 and seems to be associated with an offset of Unit 8 of 8 cm of amplitude (Fig. 5b). Fault E
345 bounds Unit 9.

346

347 *3.5. Sequence of events*

348 Retrodeformation analysis involves restoring stratigraphic units to their (inferred) original
349 geometries by graphically reversing the sense of displacement on faults. Eight rupture events
350 were recognized in the trench according to the markers of fault motions associated with the
351 deposition of units and their respective deformations (Fig. 7). Rupture events have contributed
352 to the incremental widening of the graben. According to the paleoseismological analysis, each
353 event is characterized by (potentially coseismic) displacements along one to four secondary,
354 normal faults (Fig. 7). Potential co-seismic displacements are generally in the range of 3 to 25
355 cm along the faults.

356 A first surface rupture (E1) created two antithetic normal faults B and C located currently in
357 the middle of the graben (Figs. 5 and 7). The faults were initiated into the pedogenic marl
358 (U2) and produced a graben 50 cm wide, filled by Unit 3. The constant thickness of Unit 3 (3
359 cm) provides a minimum of motion during E1 along the faults B and C. This rupture event
360 occurred before Unit 3 deposition (Fig. 7).

361 The presence of Unit 4 bounded by Fault A, in contrast to Unit 3 limited by Fault B to the
362 south, implies a new rupture event. Event 2 (E2) reactivated faults B and C, and produced a
363 new north-dipping fault (fault A) enlarging the graben on the southern side. The graben was
364 filled with Unit 4 deposit in two depocenters: (1) The southern one corresponds to a half fan-
365 shaped graben with 8 cm maximum depth and bounded by fault A: this depth corresponds to
366 the minimum offset produced along fault A during Event E2; (2) The northern depocenter is
367 filled with 7 cm-thick Unit 4 implying a minimum offset of 7 cm along faults B and C. Event
368 E2 occurred before deposition of Unit 4 dated between 778-1211 A.D., and after deposition of
369 Unit 3.

370 The third recorded event (E3) allowed the sedimentation of the 9 cm-thick Unit 5 between
371 faults A and C, sealing Fault B. Event E3 thus reactivated faults A and C with a minimum

372 displacement of 9 cm (Fig. 7). Event E3 occurred after the deposition of Unit 4, dated
373 between 778-1211 A.D. and prior to the sedimentation of Unit 5.

374 Because Unit 6, in contrast to Unit 5, has a colluvial wedge geometry another rupture event
375 after Unit 5 deposition was needed to create a new fault scarp. This Event 4 (E4) occurred
376 prior to the asymmetric deposition of Unit 6 north of Fault A. The southward thickening of
377 Unit 6 to 21 cm toward fault A suggests a tilting of Unit 5 produced by a minimum offset of
378 21 cm along Fault A during E4. Northward, Fault C could have been also reactivated as it
379 bounds a 4 cm-thick lower part of Unit 6. This measure could correspond to the minimum
380 offset on Fault C during this event.

381 A new event rupture must be inferred after Unit 6 deposition because a new unit (Unit 7)
382 appears only to the north of Fault B. To allow this sedimentation, Event 5 (E5) must have
383 produced new displacements along Fault B that offsets Units 6 and 5, creating Fault D that
384 enlarged the graben towards the north. Motion along these faults (B and D) allowed the
385 deposition of Unit 7 sealed by Unit 8. Consequently, E5 occurred between the deposition of
386 Units 6 and 8 and is therefore older than 1779 A.D. (maximum age of U8). The thickness of
387 this unit gives a minimum offset during Event 5 (E5) of 12 cm and 7 cm along faults B and D,
388 respectively. This is in agreement with the difference of offsets of Units 8 and 6 (30-17cm)
389 along fault B.

390 Several offsets of Unit 8, and the colluvial wedge geometry of Unit 9 near Fault E, indicate a
391 new rupture event. Event 6 (E6) affected Unit 8, reactivating faults A, B and D, and initiating
392 Fault E. It produced drag-folds of Unit 8 along faults A and E. The induced depression
393 between them was filled with Unit 9. Thus, this event occurred between the deposition of Unit
394 8 after 1727 AD and the deposition of Unit 9. The thickness of Unit 9 near Fault E gives a
395 minimum offset on fault E of 25 cm during Event 6 (E6) or (E5). Unit 9 near Fault A and the
396 drag-fold of Unit 8 has a thickness of 3 cm. This value is the minimum offset on Fault A
397 during Event E6 or E5 (Fig. 7). Event E6 or E4 also produced a vertical offset of 6 cm (17 cm
398 – 11 cm of U8 and U9 total offset, respectively) along Fault B and the folding of 8 cm of
399 amplitude of Unit 8 by motion along Fault D. These offsets are sealed by Unit 9.

400 According to the location of Unit 10 near the free surface of the steep scarp of Fault A with a
401 thickness decreasing moving away from the fault, a new rupture event is suggested. Event 7
402 (E7) reactivated Fault A, allowing Unit 10 deposition associated with a "Modern" sample age.
403 It is thus younger than 1750 A.D. (maximum age of unit 10, as this age is the lower boundary
404 of "plateau" process during age calibration). The thickness of Unit 10 near Fault A provides a
405 minimum offset of 15 cm on the fault during this event.

406 Because Unit 10 is slightly warped above Fault B and Unit 11 is bounded between Fault A
407 and Fault E (Fig. 4), Event 8 (E8) seems to have reactivated faults A, B and E after the
408 deposition of Unit 10 dated at a minimum of 1750 A.D. After this event, two episodes of
409 sedimentation (U11 and U12) followed. The discordance of Unit 12 on Units 10 and 11 (Fig.
410 5) and the amount of pedogenic marls coming from the surrounding Unit 2 suggest that its
411 deposition was favored by erosion. Finally a surface layer of 40 cm-thick seals all the layers
412 of the graben. It formed after the agricultural reform in 1963 A.D. Consequently, this date
413 would be the maximum age of events 6, 7 and 8.

414

415 **4. Discussion**

416 *4.1. Correlations between rupture events and historical events*

417 The young ages of the determined rupture events allow comparison between them and the
418 record of historical earthquakes near Algiers (Fig. 8). The historical record of felt earthquakes
419 in the Algiers region extends discontinuously back over 700 y (Rothé, 1950; Roussel, 1973;
420 Benhallou, 1985; Ambraseys and Vogt, 1988; Mokrane al., 1994, Yelles et al., 2002;
421 Benouar, 2004; Harbi et al., 2007a; Sebaï and Bernard, 2008; Hamdache et al., 2010). Only
422 historical events in the region associated with intensity greater than VIII and historical
423 earthquakes of intensity equal to IX or X were considered (Fig. 8). This selection was made to
424 consider only potential historical earthquakes associated with fault rupture with a magnitude
425 larger than 5.5 (McCalpin, 2009). Even if the relation between intensity and magnitude is
426 very difficult to assess, depending on several parameters, historical earthquakes with intensity
427 of VIII could potentially mean a magnitude larger than 5.5 (Gere and Shah, 1984). However,
428 a distinction was made between large historical earthquakes (*I*: IX-X) and moderate historical
429 earthquakes (*I*: VIII), the first being more favorable to generate surface ruptures and thus to
430 be recorded in the paleoseismologic trench. Unambiguous historical earthquakes are also
431 distinguished from earthquakes associated with a doubtful location (Fig. 8).

432 Events 1 and 2 predate U4 deposition. Since U4 predates U7, younger than 1171-1211 AD,
433 these two events must have occurred before 1211 AD. If U4 deposition occurred
434 consecutively and shortly after Event 2 in order to fill the graben produced by fault motion by
435 slope leaching, Event 2 must have occurred between 778 and 1211 AD, the range age of Unit
436 4. However, reliable historical accounts of earthquake activity in Algiers region prior to this
437 period are unavailable. This lack of historical data is due to the disrupted history of Algeria
438 between the 8th and 15th centuries. Before 1453 AD and the Ottoman Empire colonisation,
439 several Muslim dynasties followed one another in the region after 776 AD. This permanent

440 instability of authority prevented the conservation of ancient archives of the region (Harbi et
441 al., 2007a).

442 The following events (E3, E4 and E5) occurred between the deposition of U4 and U7.
443 Because the maximum age of U4 is 778 AD and the minimum age of U7 is 1727 AD, the
444 three events occurred between 1211 AD and 1727 AD. During this period, three significant
445 historical earthquakes and two doubtful events with intensity over VIII could have produced
446 surface ruptures (Fig 8). They occurred on January 3, 1365 (*I*: X), September 22, 1522 (*I*: IX),
447 December 31, 1658 (*I*: VIII), May 10, 1673 (*I*: VIII) and February 3, 1716 (*I*: IX-X) (Event A
448 to E, Fig. 8) (Harbi et al., 2007a). The 1522 Tipaza earthquake, which magnitude is estimated
449 at ~6.5 (Hamdache et al., 2010), is considered as doubtful because it occurred the same day as
450 the Almeria earthquake, off Spain, with a magnitude of more than 6.5 (Reicherter and Becker-
451 Heidmann, 2009). The first large historical earthquake in 1365 is often listed in historical
452 earthquake catalogs and is well-documented. It caused great damage and produced a tsunami
453 and flooding in Algiers. The 1716 earthquake is known as the strongest event that occurred in
454 Algiers during historical times. This earthquake destroyed the city of Algiers, overturning 2/3
455 of houses and damaging the remaining ones (Ambraseys and Vogt, 1988; Harbi et al., 2007a).
456 Due to their location (Fig. 1) and their intensity, these two earthquakes are good candidates to
457 correspond to one of the rupture events E3, E4 and E5. However, without more precise unit
458 dating, unambiguous correlation of one rupture event with one known historical earthquake is
459 not possible. Event 5 could have occurred just before Unit 7 deposition, as the deep fault
460 scarp B bounding the unit seems protected against erosion. As U7 range age is between 1171
461 and 1779 A.D., the same range age is suggested for Event 5, with a potential link of both
462 events with the reported historical earthquakes.

463 Events 6, 7 and 8 postdate Unit 8 deposition, younger than 1727-1779 AD and before the
464 agricultural reform in 1963 AD. During this period (1727-1963), only one certain historical
465 earthquake happened, on December 4, 1842 (*I*: VIII) (Event G, Fig. 8), and two doubtful
466 events are presumed to have occurred in 1804 (*I*: IX) (Event F, Fig. 8) and 1860 (*I*: VIII)
467 (Event H, Fig. 8). Additionally, catalogs report another earthquake that destroyed Kolea on
468 November 7, 1802 (Sebaï, 1997). Consequently, it is difficult to attempt a correlation.
469 However, as only the 1842 event is certain, it could correspond to one of the three recent
470 surface rupture events.

471

472 *4.2. Record of rupture events associated with the Sahel fault motion and interval recurrence*

473 There is evidence for eight surface-rupturing events in the analysis of the stratigraphic
474 exposure of the Kolea trench, with six ruptures produced after 778 AD. The close interaction
475 between sedimentation, erosion, and tectonic processes requires caution in paleoseismological
476 analysis. The erosion does not discount the possibility that some paleo-events were not
477 recorded in this trench, as slip may significantly change from one place to another, and
478 because ruptures during moderate- or even large-size events on this fault did not necessarily
479 reach the surface at this place. It is therefore likely that this paleoearthquake record of the
480 Sahel structure is partial. Furthermore, McCalpin et al. (2011) have shown that not every
481 thrusting event is unambiguously expressed as bending-moment displacement in the break
482 zone. This potential gap of data increases with the fact that the trench does not span the entire
483 width of the deformation zone.

484 Consequently, the incomplete paleoseismicity record of the Sahel fault activity and the youth
485 of events prevent determination of a well-constrained recurrence interval of major
486 earthquakes associated with the Sahel structure. However, three unambiguous rupture events
487 occurred between 778 A.D. and 1727 A.D. (E3 or E3' and E5 or E4'), implying a theoretical
488 recurrence interval of around 300 y. The three younger rupture episodes between 1727 AD
489 and 1963 AD indicate an interval three to four times shorter. This discrepancy could be
490 explained in different ways: (1) the lack of dating for some units may mean that the lower age
491 boundary of Event 3 is more recent than 778 AD; (2) some clustering events are major
492 paleoearthquakes followed by aftershocks and relaxation of the structure; or (3) the Sahel
493 structure has undergone a recent pulse of activity. This latter hypothesis agrees with the
494 conclusion made according to the paleoseismological analysis of the El Asnam thrust fault
495 reactivated during the October 10, 1980 event (Philip and Meghraoui, 1983; Meghraoui and
496 al., 1988), where clusters of large seismic events appear around 4000 BP and during the last
497 1000 y, separated by a quiescent period of ca. 1800 y. This particular seismogenic fault
498 behavior could also apply to the Sahel structure. However, as the trench does not span the
499 major thrust, co-seismic displacements along this fault during detected rupture events are
500 unknown and prevent estimation of the magnitude associated with these paleo-earthquakes.

501

502 **5. Conclusion**

503 This paper has presented the first paleoseismological study along the Sahel structure, and the
504 second in Algeria since the 10 October 1980 El Asnam earthquake (Ms: 7.3), which was
505 associated with the best-documented example of seismic compressive structure in North

506 Africa, combining coseismic folding, thrust faulting and secondary extrados normal faulting
507 (King and Vita-Finzi, 1981; Philip and Megharoui 1983; Meghraoui, 1988).

508 The purpose of the study was to establish the first record of paleoseismic events associated
509 with the Sahel compressive structure. The trench was dug in the hanging wall of the Sahel
510 blind thrust, where bending-moment normal faults produced by flexural slip folding were
511 encountered. The logging of the trench (Fig. 5) was made manually and the retro-deformation
512 analysis (Fig. 7) provides evidence for eight surface ruptures. Two events are older than 1211
513 AD, three events occurred between 778 AD and 1779 AD, and three are younger than 1727
514 A.D. Thus, two events are older than the older known historical earthquake (the 1365 Algiers
515 event of X intensity) and three rupture events have range ages compatible with the famous
516 1365 and 1716 Algiers historical events. The younger ruptures events forms a pulse that could
517 be interpreted as effect of one major earthquake followed by aftershocks or relaxation of the
518 structure, or a recent increase of the Sahel structure activity that favors the concept of a
519 periodicity of ruptures, a behavior already suggested in the case of the El Asnam fault
520 (Meghraoui et al., 1988). Although no accurate return periods can be inferred from the
521 observations on the secondary fault system, the results suggest that mean recurrence interval
522 is of the order of 200-250 years over recent times (i.e., since 1 ka).

523 Although this study provides preliminary paleoseismological data of the Sahel structure,
524 important issues remain open, such as estimates of the recurrence intervals of major events
525 over a longer time span, and magnitude or coseismic slip variability. Direct trenching of the
526 main Sahel thrust fault would be a critical issue in the future in order to determine the
527 magnitude of paleoearthquakes, provided the rupture zone is not too deep. Future trenches
528 and more measurements across the entire zone of surface deformation may provide answers to
529 these issues, and appear thus to have the potential to significantly improve knowledge of the
530 seismic hazards in the area of Algiers.

531

532 *Acknowledgements*

533 This work was supported by the Algerian Research Center in Astrophysics, Astronomy and
534 Geophysics (CRAAG), and was partially funded by the French CNES-TOSCA project. The
535 authors would like to thank Prof. dr hab. Tomasz Goslar from Poznań Radiocarbon
536 Laboratory in Poland for his help in the dating, as well as the inhabitants and the local
537 authorities of Kolea city (Algeria) for their help. We thank the anonymous reviewer for
538 comments which improved the manuscript.

539

540 **References**

- 541 Ambraseys, N., Vogt, J., 1988. Material for the investigation of the seismicity of the region of
542 Algiers. *European Earthquake Engineering* 3, 16-29.
- 543 Anderson, H., Jackson, J., 1987. Active tectonics of the Adriatic Region. *Geophysical Journal*
544 *of the Royal Astronomical Society* 91: 937–983. doi: 10.1111/j.1365246X. 1987. Tb
545 01675. x.
- 546 Ayadi, A., and 27 authors, 2003. Strong Algerian earthquake strikes near capital city. *Eos,*
547 *Transactions, AGU* 84, 50, 561- 568.
- 548 Ayadi, A., Dorbath, C., Ousadou, F., Maouche, S., Chikh, M., Bounif, M.A., Meghraoui, M.,
549 2008. Zemmouri earthquake rupture zone (Mw 6.8, Algeria): Aftershocks sequence
550 relocation and 3D velocity model. *Journal of Geophysical Research* 113, B09301,
551 doi:10.1029/2007JB005257.
- 552 Aymé, A., 1952. Le quaternaire littoral des environs d'Alger. *Proceeding of the Pan-African*
553 *Congress of Prehistory, Session II. Algiers, Algeria, pp. 243–245.*
- 554 Aymé, A., Aymé, J. M., Magné, J., 1954. Etude des terrains néogènes de la cluse de Mazafran
555 (Sahel d'Alger). *Travaux des collaborateurs. Bulletin n° 1, Fascicle 11, 129- 150.*
- 556 Beldjoudi, H., Delouis, B., Heddar, A., Nouar, O., Yelles-Chaouche, A., 2011. The Tadjena
557 Earthquake (Mw = 5.0) of December 16, 2006 in the Cheliff Region (Northern Algeria):
558 Waveform Modelling, Regional Stresses, and Relation with the Boukadir Fault. *Pure and*
559 *Applied Geophysics, Doi: 10.1007/s00024-011-0337-8.*
- 560 Belhai, D., 1987. Massif du Chenoua (Algérie): mise en place des flyschs en relation avec un
561 cisaillement dextre transcurrent EW responsable de la structure en éventail. *Magister*
562 *Thesis, Science and Technology Houari Boumédiène University of Algiers, Algeria*
- 563 Belhai, D., Merle, O., Saadallah, A., 1990. Transpression dextre à l'Éocène supérieur dans la
564 chaîne des Maghrébides (massif du Chenoua, Algérie). *Comptes Rendus de l'Académie*
565 *des Sciences, Paris, Série 2, 310 (06), 795 - 800.*
- 566 Benhallou, H., Ferrer, A. and Roussel, J., 1971. Catalogue des séismes algériens de 1951 à
567 1970. *Institut de Météorologie et de Physique du Globe de l'Algérie (IMPGA).*
568 *University of Algiers, Algeria*
- 569 Benhallou, H., 1985. Les catastrophes sismiques de la région d'Echelif dans le contexte de la
570 sismicité de l'Algérie. *Ph.D. Thesis, Science and Technology Houari Boumédiène*
571 *University of Algiers, Algeria*
- 572 Benouar, D., 1994. Materials for the investigation of the seismicity of Algeria and adjacent
573 regions during the twentieth century. *Special Issue of Annali di Geofisica, 37, 459-860.*

- 574 Berberian, M., 1979. Earthquake faulting and bedding thrust associated with the Tabas e
575 Goldshan (Iran) earthquake of December 16, 1978. *Bulletin Seismological Society of*
576 *America* 69, 1861-1887.
- 577 Bessaoud, O., 1980. La révolution agraire en Algérie: continuité et rupture dans le processus
578 de transformations agraires. *Tiers-Monde* 21, 605-626.
- 579 Bezzeghoud, M., Ayadi, A., Sebaï, A., Ait Messaoud, A., Mokrane, A., and Benhallou, H.,
580 1996. Seismicity of Algeria between 1365 and 1989: Map of Maximum observed
581 intensities (MOI), *Avances en Geofisica y Geodesia* 1, ano 1, Ministerio de Obras
582 Publicas, Transportes y Medio Ambiente, Instituto Geografico National España, 107-114.
- 583 Blès, J –L., 1971. Etude tectonique et microtectonique d'un massif autochtone tellien et sa
584 couverture de nappes : le massif de Blida (Algérie du Nord). *Bulletin de la Société*
585 *Géologique de France* 13 (5-6), 498-511.
- 586 Bonneton, J. R., 1977. Géologie de la zone de contact entre la Mitidja et l'Atlas de Blida au
587 sud d'Alger. Ph.D. Thesis, Pierre and Marie Curie University of Paris, France
- 588 Boudiaf, A., 1996. Etude sismotéctonique de la région d'Alger et de la Kabylie (Algérie):
589 Utilisation des modèles numériques de terrain (MNT) et de la télédétection pour la
590 reconnaissance des structures tectoniques actives: contribution à l'évaluation de l'aléa
591 sismique. Ph.D. Thesis, Montpellier II University, France
- 592 Bounif, A., Bezzeghoud, M., Dorbath, L., Legrand, D., Deschamps, A., Rivera, L. and
593 Benhallou, H., 2003. Seismic source study of the 1989, October, Chenoua (Algeria)
594 earthquake from aftershocks, broad-band and strong ground motion records. *Annals of*
595 *Geophysics* 46 (4), 625-646.
- 596 Bounif, A., Dorbath, C., Ayadi, A., Meghraoui, M., Beldjoudi, H., Laouami, N., Frogneux,
597 M., Slimani, A., Alasset, J.P., Kharroubi, A., Oussadou, F., Chikh, M., Harbi, A., Larbes,
598 S., Maouche, S., 2004. The 21 May, 2003. (Mw 6.8) Zemmouri (Algeria) earthquake
599 relocation and aftershock sequence analysis. *Geophysical Research Letters* 31, L19606,
600 doi:10.1029/2004GL020586.
- 601 Carminati, E., Wortel, M. J. R., Spakman, W., Sabadini, R., 1998. The role of slab
602 detachment process in the opening of the western central Mediterranean basins: Some
603 geological and geophysical evidence. *Earth and Planetary Science Letters*. 160, 651–665.
- 604 De Lamothe, G., 1911. Les anciennes lignes de rivage du Sahel d'Alger et d'une partie de la
605 côte Algérienne. *Memoires de la Société Géologique de France*, 4eme Série, I, Mémoire
606 N° 6.

- 607 DeMets, C., Gordon, R., Argus, D.F., Stein, S., 1990. Current plate motions. *Geophysical*
608 *Journal International* 181, 425-478.
- 609 Deschamps, A., Gaudemer, Y. and Cisternas, A., 1982. The El Asnam, Algeria, earthquake
610 of 10 October 1980: multiple source mechanism determined from long period record.
611 *Bulletin of the Seismological Society of America* 72, 1111–1128.
- 612 Déverchère, J., Yelles, K., Domzig, A., Mercier de Lépinay, B., Bouillin, J.P., Gaullier, V.,
613 Bracène, R., Calais, E., Savoye, B., Kherroubi, A., Le Roy, P., Pauc, H., Dan, G., 2005.
614 Active thrust faulting offshore Boumerdes, Algeria, and its relations to the 2003 Mw 6.9
615 earthquake. *Geophysical Research Letters* 32, L04311, doi: 10.1029/2004GL021646.
- 616 Déverchère, J., Mercier de Lepinay, B., Cattaneo, A., Strzeczynski, P., Calais, E., Domzig,
617 A., Bracene, R., 2010. Comment on "Zemmouri earthquake rupture zone (Mw 6.8,
618 Algeria): aftershocks sequence relocation and 3D velocity model" by Ayadi et al. *Journal*
619 *of Geophysical Research* 115, B04320, doi: 10.1029/2008JB006190.
- 620 Domzig, A., 2006. Déformation active et récente, et structuration tectonosédimentaire de la
621 marge sous-marine algérienne. Ph.D. Thesis, University of Western Brittany, France
- 622 Domzig, A., Yelles A-K., Le Roy, C., Déverchère, J., Bouillin, J.-P., Bracene, R., Mercier de
623 Lépinay, B., Le Roy P., Calais, E., Kherroubi, A., Gaullier, V., Savoye, B. and Pauc, H.,
624 2006. Searching for the Africa-Eurasia Miocène boundary offshore western Algeria
625 (MARADJA'03 cruise). *Comptes Rendus Geoscience* 338, 80-91.
- 626 Duggen, S., Hoernle, K., Van den Bogaard, P., Harris, C., 2004. Magmatic evolution of the
627 Alboran region: The role of subduction in forming the western Mediterranean and
628 causing the Messinian Salinity Crisis, *Earth and Planetary Science Letters* 218, 91-108.
- 629 Durand-Delga, M., 1969. Mise au point sur la structure du Nord-Est de la Berberie. *Bulletin*
630 *of Geological Algeria Card Service*, 39, 89-131.
- 631 Frizon De Lamotte, D., Saint Bezar, B., Bracene, R., Mercier, E., 2000. The two main steps of
632 the Atlas building and geodynamics of the western Mediterranean. *Tectonics* 19, 740-
633 761.
- 634 Gere, J. M., Shah, H. C., 1984. *Terra non firma: Understanding and preparing for*
635 *earthquakes*. Freeman, New York, USA
- 636 Glangeaud, L., 1932. *Etude géologique de la région littorale de la province d'Alger*. Book
637 Edited by Cadoret Y., 1932, Bordeaux, France
- 638 Glangeaud, L., Aymé, A., Caire, A., Mattauer, M., et Miraour, P., 1952. *Histoire géologique*
639 *de la province d'Alger*. XIX international geological congress Algiers, regional
640 *Monographs first series, Algeria*, 141 pp.

- 641 Guemache, M. A., 2010. Evolution géodynamique des bassins sismogènes de l'Algérois
642 (Algérie) Approche pluridisciplinaire (Méthodes Géologiques et Géophysiques), Ph.D.
643 Thesis, Science and Technology Houari Boumédiène University of Algiers, Algeria
- 644 Guemache, M. A., Djellit, H., Ymmel, H., Gharbi, S., Dorbath, C., 2010. The Post-Astian
645 Bouinan–Soumâa fault (area of Blida, Southern border of the Mitidja Basin, Algeria):
646 Neotectonic expression and implication in seismic hazard assessment. Bulletin of
647 Geological Algeria Card Service, 21(1), 75-94.
- 648 Gueguen, E., Doglioni, C., Fernandez, M., 1998. On the post-25 Ma geodynamic evolution of
649 the western Mediterranean. Tectonophysics 298, 259–269.
- 650 Hamai, L., 2011. Etude gravimétrique de la Mitidja Occidentale, memory magister
651 geophysics, Science and Technology Houari Boumédiène University of Algiers, Algeria
- 652 Hamdache, M., Peláez, J.A., Talbi, A., López Casado, C., 2010. A Unified Catalog of Main
653 Earthquakes for Northern Algeria from A.D. 856 to 2008. Seismological Research Letters
654 81 (5),732-739.
- 655 Harbi, A., 2006. Evaluation de l'aléa sismique en Algérie du nord par la modélisation de
656 l'input sismique dans les zones urbaines et l'établissement d'un catalogue. Ph.D. Thesis,
657 Science and Technology Houari Boumédiène University of Algiers, Algeria
- 658 Harbi, A., Maouche, S., Ayadi, A., Benouar, D., Panza, G.F., Benhallou, H., 2004. Seismicity
659 and tectonics structures in the site of Algiers and its surroundings: A step towards
660 microzonation. Pure and applied geophysics, 161, 949-967.
- 661 Harbi, A., Maouche, S., Vaccari, F., Aoudia, A., Oussadou, F., Panza, G.F., Benouar, D.,
662 2007a. Seismicity, Seismic Input and Site effects in the Sahel-Algiers Region (North
663 Algeria). Soil Dynamics and Earthquake Engineering 27 (5), 427-447.
- 664 Harbi, A., Maouche, S., Ousadou, F., Rouchiche, Y., Yelles-Chaouche, A., Merahi, M.,
665 Heddar, A., Nouar, O., Kherroubi, A., Beldjoudi, H., Ayadi, A., Benouar, D., 2007 b.
666 Macroseismic study of the Zemmouri Earthquake 21 May 2003 (Mw 6.8, Algeria).
667 Earthquake Spectra 23 (2), 315-332.
- 668 Hée, A., 1950. Catalogue des séismes algériens de 1850 à 1911. Annales de l'Institut de
669 Physique du Globe, Strasbourg, 6, 41-49, France
- 670 Higgins, C., Coates, D. R., 1990. Groundwater and geomorphology, the role of subsurface
671 water in Earth-surface processes and landforms. Geological Society of America Special
672 Paper, 252, 368pp.
- 673 Jolivet, L., Faccenna, C., 2000. Mediterranean extension and Africa-Eurasia collision.
674 Tectonics 19 (6), 1095-1106.

- 675 King, G.C.P. and Vita-Finzi, C., 1981. Active folding in the Algerian earthquake of 10
676 October 1980, *Nature* 292, 22–26.
- 677 Maouche, S., Benouar, D., Harbi, A., Benhallou, H., 1998. The Algiers (Algeria) Earthquake
678 of 4 September 1996. *European Earthquake Engineering journal*, 10 (1), 51-55.
- 679 Maouche, S., Meghraoui, M., Morhange, C., Belabbes, S., Bouhadad, Y., Haddoum, H., 2011.
680 Active coastal thrusting and folding, and uplift rate of the Sahel Anticline and Zemmouri
681 earthquake area (Tell Atlas, Algeria). *Tectonophysics* 509(1-2), 69-80.
- 682 Mauffret, A., Frizon de Lamotte, D., Lallemand, S., Gorini, G., Maillard, A., 2004. E-W
683 opening of the Algerian Basin (West Mediterranean). *Terra Nova* 16, 257-264.
- 684 McCalpin, J. P., 2009. *Paleoseismology*, 2nd ed., International Geophysics Series, Academic
685 Press, London, 613pp.
- 686 McCalpin, J. P., Bruhn, R. L., Pavlis, T. L., Gutierrez, F., Guerrero, J., Lucha, P., 2011.
687 Antislope scarps, gravitational spreading, and tectonic faulting in the western Yakutat
688 microplate, south coastal Alaska. *Geosphere*, 7, 1143-1158.
- 689 Meghraoui, M., 1988. *Géologie des zones sismiques du nord de l'Algérie (Paléosismologie,*
690 *Tectonique active et synthèse sismotectonique)*. Ph.D. Thesis, Paris-Sud University,
691 Centre d'Orsay, France
- 692 Meghraoui, M., 1991. Blind reverse faulting system associated with the Mont Chenoua-
693 Tipasa earthquake of 29 October 1989 (north-central Algeria). *Terra Nova* 3, 84-93.
- 694 Meghraoui, M., Philip, H., Albarede, F., Cisternas, A., 1988. Trench investigations through
695 the trace of the 1980 El Asnam thrust fault: evidence from paleoseismicity. *Bulletin of*
696 *the Seismological Society of America* 78(2), 979-999.
- 697 Meghraoui, M., Maouche, S., Chemaï, B., Cakir, Z., Aoudia, A., Harbi, A., Alasset, P-J.,
698 Ayadi, A., Bouhadad, Y., Benhamouda, F., 2004. Coastal uplift and thrust faulting
699 associated with the Mw=6. 8 Zemmouri, (Algeria) earthquake of 21 May 2003.
700 *Geophysical Research Letters*, 31, L19605, doi: 10. 1029/2004GL020466.
- 701 Mokrane, A., Ait Messaoud, A., Sebaï, A., Ayadi, A., Bezzeghoud, M., Benhallou, H., 1994.
702 *Les séismes en Algérie de 1365 à 1992*. Publication du Centre de Recherche en
703 *Astronomie, Astrophysique et Géophysique (C.R.A.A.G)*, Algiers, Algeria. 277 pp.
- 704 Oussadou, F., 2002. *Contribution à la sismotectonique de l'Algérie occidentale par la*
705 *sismicité, les mécanismes au foyer, les mesures de déformation et la tectonique générale.*
706 *Memory magister geophysics*, Science and Technology Houari Boumédienne University
707 of Algiers, Algeria

- 708 Ouyed, M., Meghraoui, M., Antenor-Habazac, C., Bourezg, S., Cisternas, A., Dorel, J.,
709 Frechet, J., Frogneux, M., Hatzfeld, D., Philip, H., 1980. Le séisme d'El Asnam du 10
710 Octobre 1980, premiers résultats sismologiques et tectoniques. Comptes rendus de
711 l'Académie des sciences de Paris, Tome 291.
- 712 Ouyed, M., Meghraoui, M., Cisternas, A., Deschamps, A., Dorel, J., Frechet, J., Gaulon, R.,
713 Hatzfeld, D., Philip, H., 1981. Seismotectonics of the El Asnam earthquake. *Nature* 292,
714 26-31.
- 715 Ouyed, M., Yielding, G., Hatzfeld, D., and King, G. C. P., 1982. An aftershock study of the
716 Al-Asnam(Algeria) earthquake of 1980 October 10. *Geophysical Journal of the Royal*
717 *Astronomical Society*, 73, 605-639.
- 718 Perrey, A., 1847. Note sur les tremblements de terre en Algérie et dans l'Afrique
719 septentrionale. *Memoirs of the Academy of Sciences Arts and Belles Lettres*, Dijon,
720 France, 299-323.
- 721 Philip, H., Meghraoui, M., 1983. Structural analysis and interpretation of the surface
722 deformation of the Asnam earthquake of October 10, 1980. *Tectonics* 2, 299-349.
- 723 Reicherter, K., Becker-Heidmann, P., 2009. Tsunami deposits in the western Mediterranean:
724 remains of the 1522 Almería earthquake? *Geological Society, London, Special*
725 *Publication*, 316, 217-235.
- 726 Reimer, P. J., Baillie, M. G. L., Bard, E., Bayliss, A., Beck, J. W., Backwell, P. G., Ramsey,
727 C. B., Buck, C. E., Burr, G. S., Edwards, R. L., Friedrich, M., Grootes, P. M., Guilderson,
728 T. P., Hadas, I., Heaton, T. J., Hogg, A. G., Hughen; K. AL, Kaiser, K. F., Kromer, B.,
729 McCormac, F. G., Manning, S. W., Reimer, R. W., Richards, D. A., Southon, J. R.,
730 Talamo, S., Turney, C. S. M., Van der Plucht, J., Weyhenmeyer, C. E., 2009. IntCal09
731 and Marine09 radiocarbon age calibration curves, 0-50,000 years cal BP. *Marine*
732 *Chemistry and Geochemistry* 51, 1111-1150.
- 733 Rothé, J.P., 1950. Les Séismes de Kherrata et la simicité de l'Algérie. *Bulletin of Geological*
734 *Algeria Card Service*, 4th series, *Geophysics*, 3, pp. 40.
- 735 Rothé, J.P., 1955. Le tremblement de terre d'Orléanville et la sismicité de l'Algérie. *La*
736 *Nature*, 3237.
- 737 Roussel, J., 1973. Les zones actives et la fréquence des séismes en Algérie. *North Africa*
738 *Bulletin of Natural History Society*, 64(3/2), 11-22.
- 739 Saadallah, A., 1981. Le massif cristallophyllien d'El-Djazaïr (Algérie) : Evolution d'un
740 charriage à vergence nord dans les internides des Maghrébides. Ph.D. Thesis, Science and
741 Technology Houari Boumédiène University of Algiers, Algeria

- 742 Saoudi, N., 1989. Pliocène et Pléistocène inférieur et moyen du Sahel d'Alger. ENAG,
743 Algiers, Algeria, 174 pp.
- 744 Schettino, A., Turco, E., 2006. Plate kinematics of the Western Mediterranean region during
745 the Oligocene and Early Miocene. *Geophysical Journal International* 166, 1398-1423.
- 746 Sebaï, A., 1997. Analyse sismologique des séismes récents du Sahel d'Alger. Memory
747 magister geophysics, Science and Technology Houari Boumédiène University of
748 Algiers, Algeria
- 749 Sebaï, A., Bernard, P., 2008. Contribution à la connaissance de la sismicité d'Alger et de ses
750 alentours au XVIIIe siècle, extraite des archives françaises. *Comptes Rendus Geoscience*
751 340, 495–512.
- 752 Serpelloni, E., Vannucci, G., Pondrelli, S., Argnani, A., Casula, G., Anzidei, M., Baldi, P.,
753 Gasperini, P., 2007. Kinematics of the Western Africa-Eurasia plate boundary from focal
754 mechanisms and GPS data, *Geophysical Journal International*, 169 (3), 1180-1200.
- 755 Stich, D., Serpelloni, E., Mancilla, F. D. L., Morales, J., 2006. Kinematics of the Iberia-
756 Maghreb plate contact from seismic moment tensors and GPS observations.
757 *Tectonophysics* 426, 295–317.
- 758 Strzeczynski, P., Déverchère, J., Cattaneo, A., Domzig, A., Yelles, K., Mercier de Lépinay,
759 B., Babonneau, N. and Boudiaf, A., 2010. Tectonic inheritance and Pliocene-Pleistocene
760 inversion of the Algerian margin around Algiers: Insights from multibeam and seismic
761 reflection data. *Tectonics* 29, TC2008, doi:10.1029/2009TC002547.
- 762 Thomas, G., 1976. Mise en évidence de décrochements dextres Est-Ouest d'âge quaternaire en
763 Algérie nord occidentale. *Comptes rendus de l'Académie des sciences de Paris, France,*
764 série D 283, 893-896.
- 765 Vergès, J., Sabàt F., 1999. Constraints on the Western Mediterranean kinematics evolution
766 along a 1000-km transect from Iberia to Africa. In: B. Durant, L. Lolivet, F. Horvarth and
767 M. Séranne, ed., *The Mediterranean basin: Tertiary extensions within the Alpine orogen.*
768 *Geological Society of London, Special Publication* 156, 63-80.
- 769 Yelles-Chaouche, A.K, Deramchi A, Ferkoul, A., Aoulaiche, K., 2002. Les séismes d'Algérie
770 du Nord de 1992–2001. *Catalogue of Centre de Recherche en Astronomie, Astrophysique*
771 *et Géophysique (CRAAG), Algeria.*
- 772 Yelles, A.K., Lammali, K., Mahsas, A., 2004. Coseismic deformation of the May 21st, 2003,
773 Mw = 6.8 Boumerdes earthquake, Algeria, from GPS measurements. *Geophysical*
774 *Research Letters*, 31, L13610, doi: 10.1029/2004GL019884.

775 Yelles, A.K., Domzig, A., Déverchère, J., Bracène, R., Mercier de Lépinay, B., Strzeczynski,
 776 P., Bertrand, G., Boudiaf, A., Winter, T., Kherroubi, A., Le Roy, P., Djellit, H., 2009.
 777 Evidence for large active fault offshore west Algiers, Algeria, and seismotectonic
 778 implications. *Tectonophysics* 475, 98-116.

779 Yelles, A.K., Boudiaf, A., Djellit, H., Bracene, R., 2006. La tectonique active de la région
 780 Nord-algérienne. *Comptes Rendus Geoscience* 338, 126–139.

781 Yielding, G., Jackson, J.A., King, G.C.P., Sinvhal, H., Vita-Finzi, C. and Wood, R.M., 1981.
 782 Relations between surface deformation, fault geometry, seismicity, and rupture
 783 characteristics during the El Asnam (Algeria) earthquake of 10 October 1980. *Earth and*
 784 *Planetary Science Letters* 56, 287-305.

785

786 ***Table caption***

787 **Table 1:** measured and corrected ages of samples collected in the trench. Measured ages have
 788 been corrected for the atmospheric $^{14}\text{C}/^{13}\text{C}$ ratio over the last few millennia using IntCal, an
 789 on-line CALIB Manual 6.0 radiocarbon calibration tool hosted by the Quaternary Isotope
 790 Laboratory at the University of Washington, UK (<http://calib.qub.ac.uk>). For each sample, a
 791 probability density and a relative area under probability distribution are obtained (Reimer et
 792 al., 2009). Charcoal samples smaller than 0.2 mgC were removed because they do not give
 793 reliable ages. Samples associated with a "plateau" calibrated age were considered "Modern",
 794 corresponding to a maximum age of 1750 AD (Reimer et al., 2009).

795

796 ***Figure captions***

797 **Figure 1.** Seismotectonic map of Algiers and its surroundings. Shaded bathymetric (from
 798 MARADJA cruise) and topographic (90 m-SRTM DEM) maps showing offshore (Domzig et
 799 al., 2006; Strzeczynski et al., 2010) and onshore faults (Meghraoui, 1988; Boudiaf, 1996;
 800 Yelles et al., 2006) (lines). Focal mechanisms of main shock ($M_w > 4.9$) (Deschamps et al.,
 801 1982; Bounif et al., 2003; 2004; Beldjoudi et al., 2011; GFZ; Havard CMT) associated with
 802 epicentres of principal earthquakes after 1980 (stars). Open squares show the location of the
 803 significant historical earthquakes and dotted open squares show the location of doubtful
 804 historical earthquakes (Benouar, 1994; Harbi et al., 2007a). White dots correspond to
 805 epicentres of instrumental seismicity ($M_w > 2$) (Benouar, 1994; extraction from C.R.A.A.G.
 806 Catalogue, 1994, 2002, 2011).

807 **Figure 2.** Geological map of the Algiers region showing the Sahel ridge and faults
 808 (Strzeczynski et al., 2010; Maouche et al., 2011). B : Geological cross-section of the Sahel

809 ridge according to Maouche et al. (2011). C: Geological cross-section of the Sahel ridge
810 according to Aymé et al. (1954). For location see figure 1.

811 **Figure 3.** Views of Pliocene formations cropping out at the bottom of the southern flank of
812 the Sahel structure. A: Layers of Pliocene marls and sandstones at site 1 dipping 31° to the
813 SE. B: Layers of Upper Pliocene sandstones at site 2 dipping 84° to the SE. For location see
814 Figure 2.

815 **Figure 4.** Geomorphological and geological context of the study zone. A: A SPOT satellite
816 image (5m-resolution) indicates a morphologic scarp and the location of the cross-section in
817 Figure 5B and the trench sites shown in Figures 5, 6 and in auxiliary material. B: Geological
818 cross-section showing the relationship between the major Sahel thrust and the studied
819 secondary faults. For location see Figure 2.

820 **Figure 5.** Paleoseismological trench wall exhibiting the graben structure outcropping in the
821 southern flank of the Sahel structure. Grid has 50 cm mesh. Trench location is denoted on
822 Figures 2A and 4. A and B: detail of the trench showing deformation markers associated with
823 motion along the faults. C: View of the trench wall. B: Log of the trench. Faults are lines
824 labelled A to E. White stars indicate the age and the location of the samples dated with
825 radiocarbon analyses. Stratigraphic contacts are shown in thin black lines with encircled black
826 numbers representing the unit name. Units: 1: Quaternary conglomerates with angular pebbles
827 well consolidated in a silty matrix, 2: Quaternary white marls of alteration clay, 3, 4 and 5:
828 deposits with gravels in a silty clay matrix, 6 and 7: silty clays containing shells and detrital
829 charcoal, 8: peat horizon, 9, 10, 11 and 12: brown silty clays.

830 **Figure 6.** Outcrop of the studied zone affected by normal faults. A: Picture of the outcrop. B:
831 Interpretation of the outcrop. Location shown on Figure 4.

832 **Figure 7.** Inferred sequence of deformation, sedimentation and erosion at the trench. See text
833 for details.

834 **Figure 8.** Diagram of age ranges of paleo-events (horizontal red lines) and dates of historical
835 earthquakes (vertical thick lines: $I = VIII$; vertical thin lines: $I = IX$ or X , dotted lines are
836 doubtful earthquakes. Below the graph, certain historical earthquakes are reported in black,
837 doubtful earthquakes are reported in grey).

838

839 *Appendix*

840 Paleoseismological trench wall exhibiting alluvial deposits located on the morphological
841 scarp 200-m downward the graben structure outcropping in the southern flank of the Sahel
842 structure. Grid has 100 cm mesh. Trench location is denoted on Figure 4. A and B: View of

843 the trench wall. C: Log of the trench. Stratigraphic contacts are shown in thin black lines with
844 encircled black letters representing the unit name. Unit UA correspond to Quaternary marls.
845 Units UB to UT are alluvial units, dominantly conglomerates with some sandy horizons.
846

ACCEPTED MANUSCRIPT

Sample	Unit	Measured age BP	Calibrated AD age range	Probability %	Relative area under probability distribution	Laboratory specimen number	Specimen Detail
e1	U4	1170 ± 20	778-897	95.4 (2σ)	0.918	UGAMS 8873	Helix
e2	U6	100 ± 1	Not reliable			Poz-41032 S	Charcoal ≤0.2mgC
e3	U7	860 ± 20	1171-1211	68.3 (1σ)	1	UGAMS 08872	Helix
e4	U8	210 ± 60	Not reliable			Poz-41033 S	Charcoal ≤0.2mgC
e5	U8	150 ± 30	1727-1779	68.3 (1σ)	0.42	Poz-41039	Charcoal >0.2mgC
e6	U9	570 ± 30	1304-1365	95.4 (2σ)	0.603	Poz-41036	Charcoal >0.2mgC
e7	U9/U10	101 ± 1	Modern			Poz-41038	Charcoal >0.2mgC
e8	U10	100 ± 30	Modern			Poz-41037	Charcoal >0.2mgC
e9	U11	230 ± 70	Not reliable			Poz-41034 S	Charcoal ≤0.2mgC
e10	U12	320 ± 50	1455-1654	95.4 (2σ)	1	Poz-41040 S	Charcoal >0.2mgC
e11	soil	75 ± 50	Modern			Poz-41041	Charcoal >0.2mgC

Table 1: measured and corrected ages of samples collected in the trench. Measured ages have been corrected for the atmospheric $^{14}\text{C}/^{13}\text{C}$ ratio over the last few millenia using IntCal, an on-line CALIB Manual 6.0 radiocarbon calibration tool hosted by the Quaternary Isotope Laboratory at the University of Washington, UK (<http://calib.qub.ac.uk>). For each sample, a probability density and a relative area under probability distribution are obtained (Reimer et al., 2009). Charcoal sample smaller than 0.2 mgC were removed because that give not reliable age. Samples associated with a "plateau" calibrated age were qualified of "Modern" corresponding to a maximum age of 1750 AD (Reimer et al., 2009).

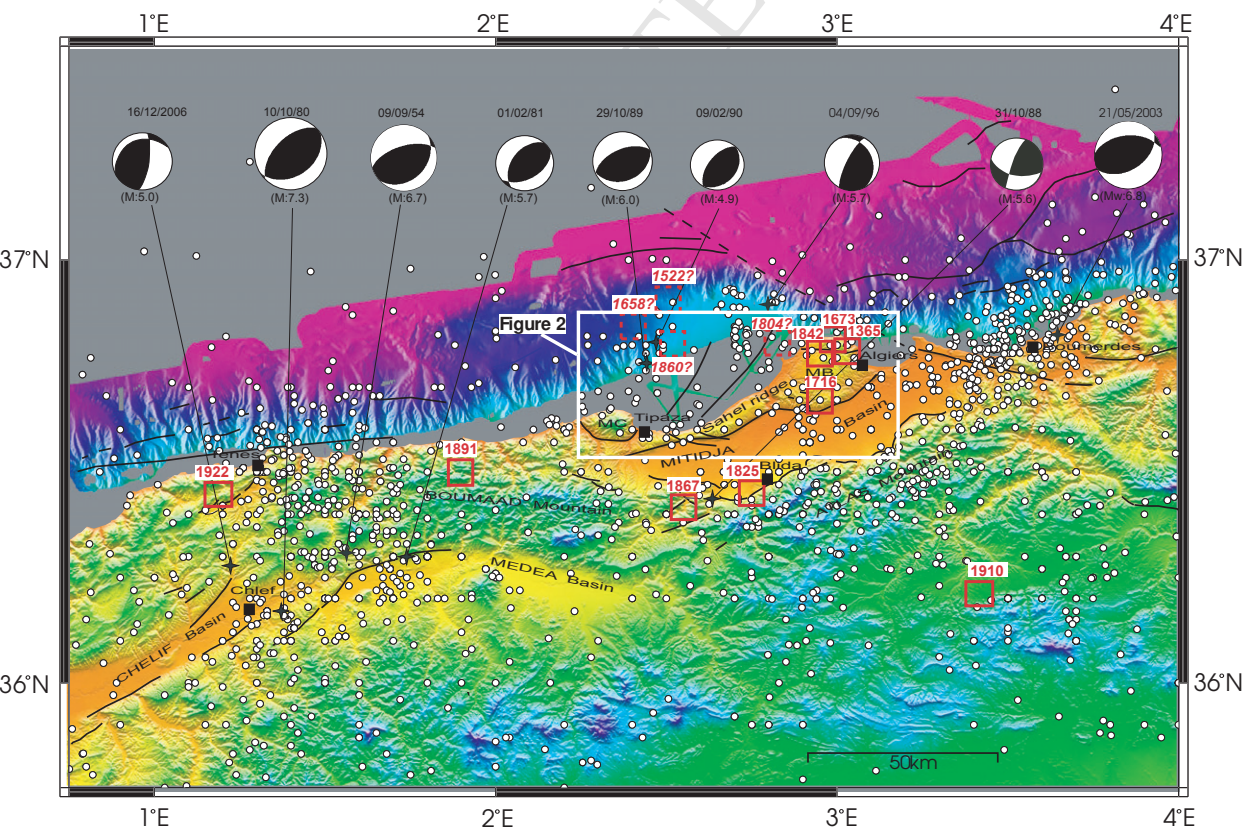


Figure 1

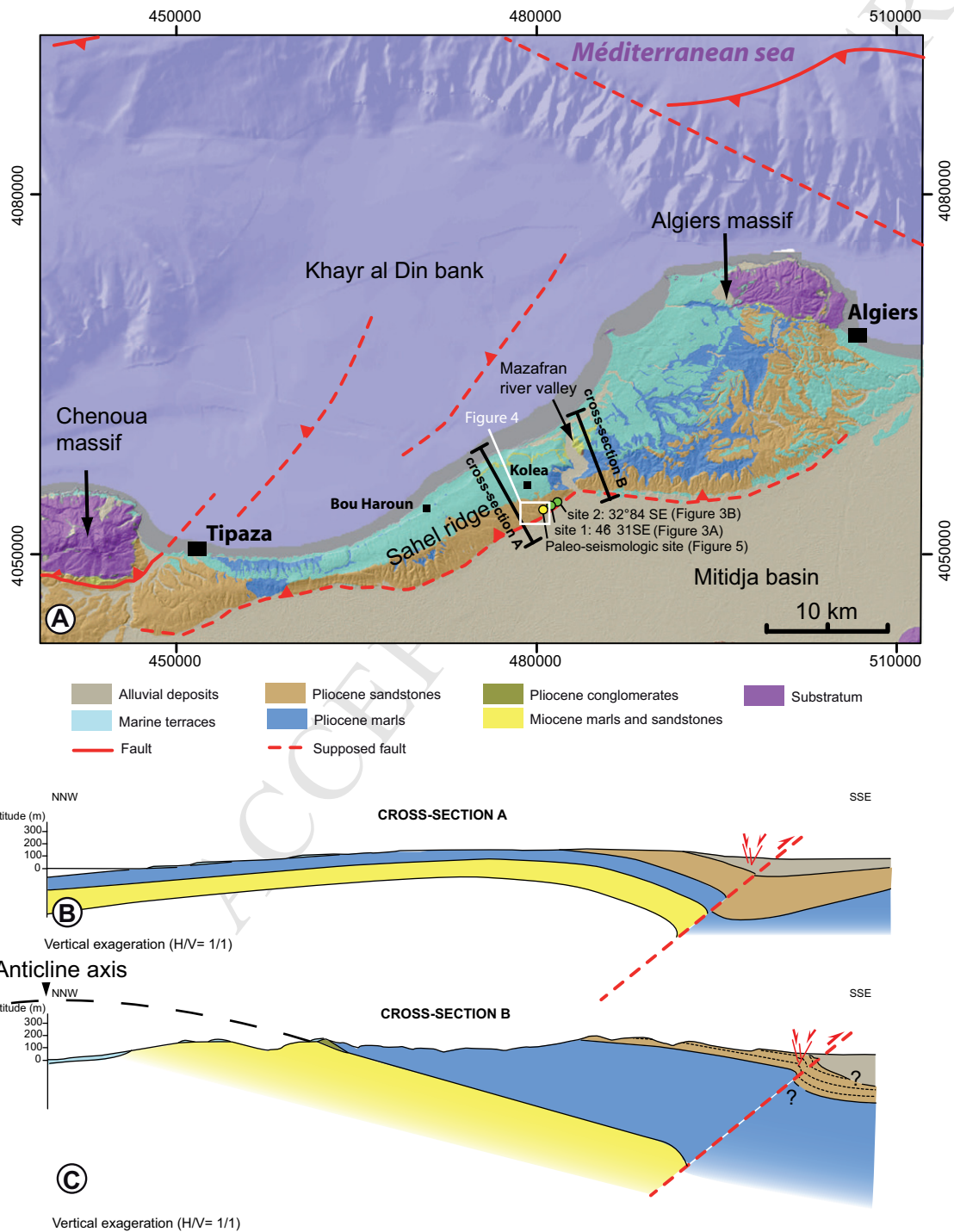


Figure 2

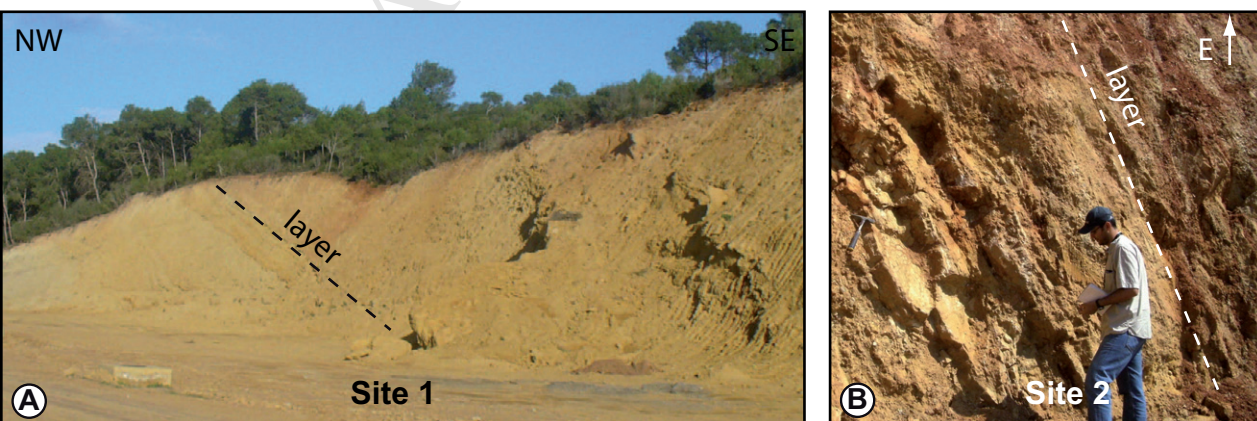
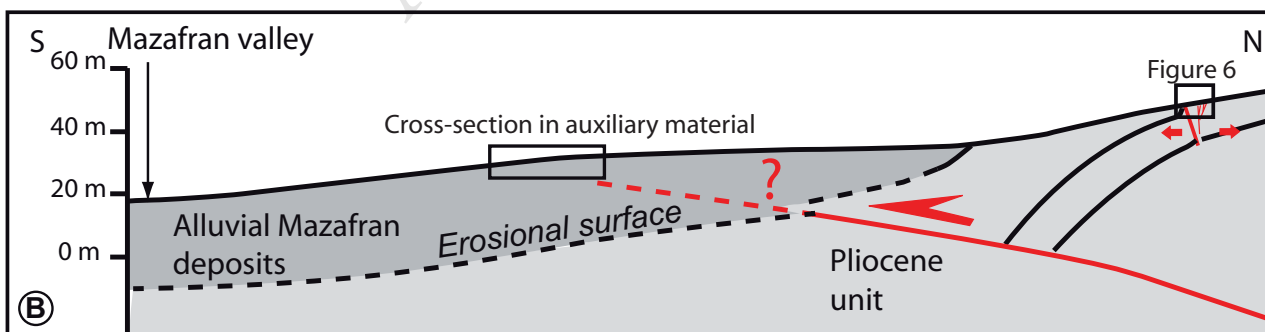
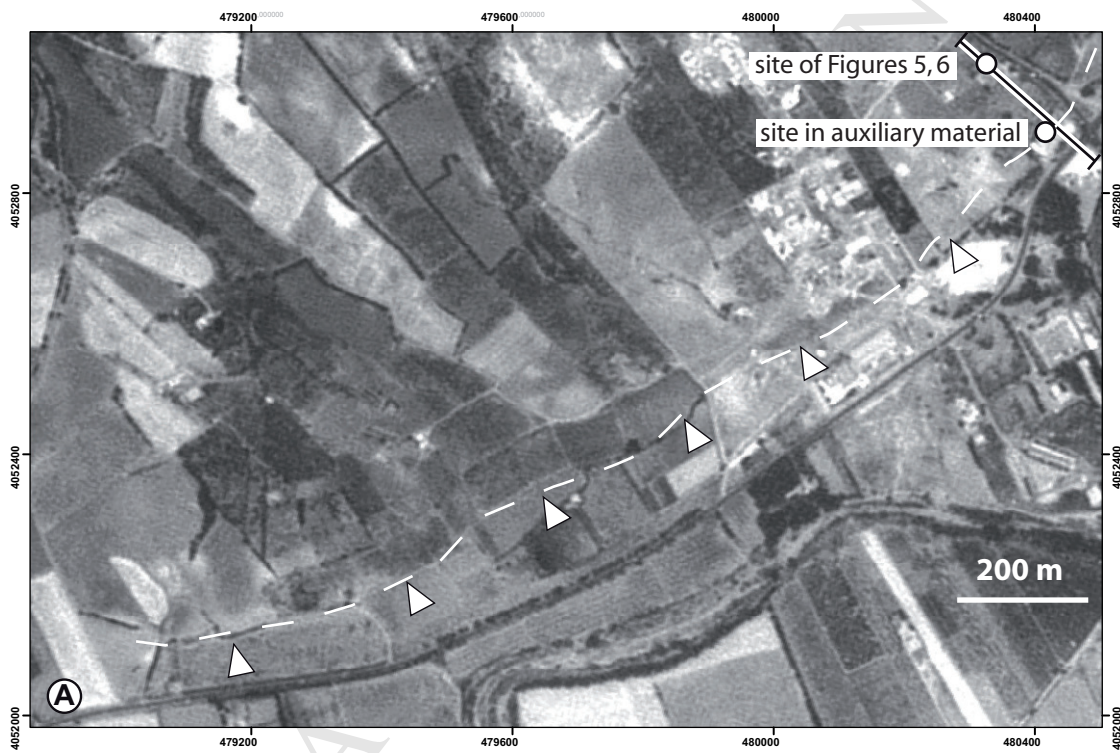


Figure 3



No vertical exaggeration ($H/V = 1/1$)

Figure 4

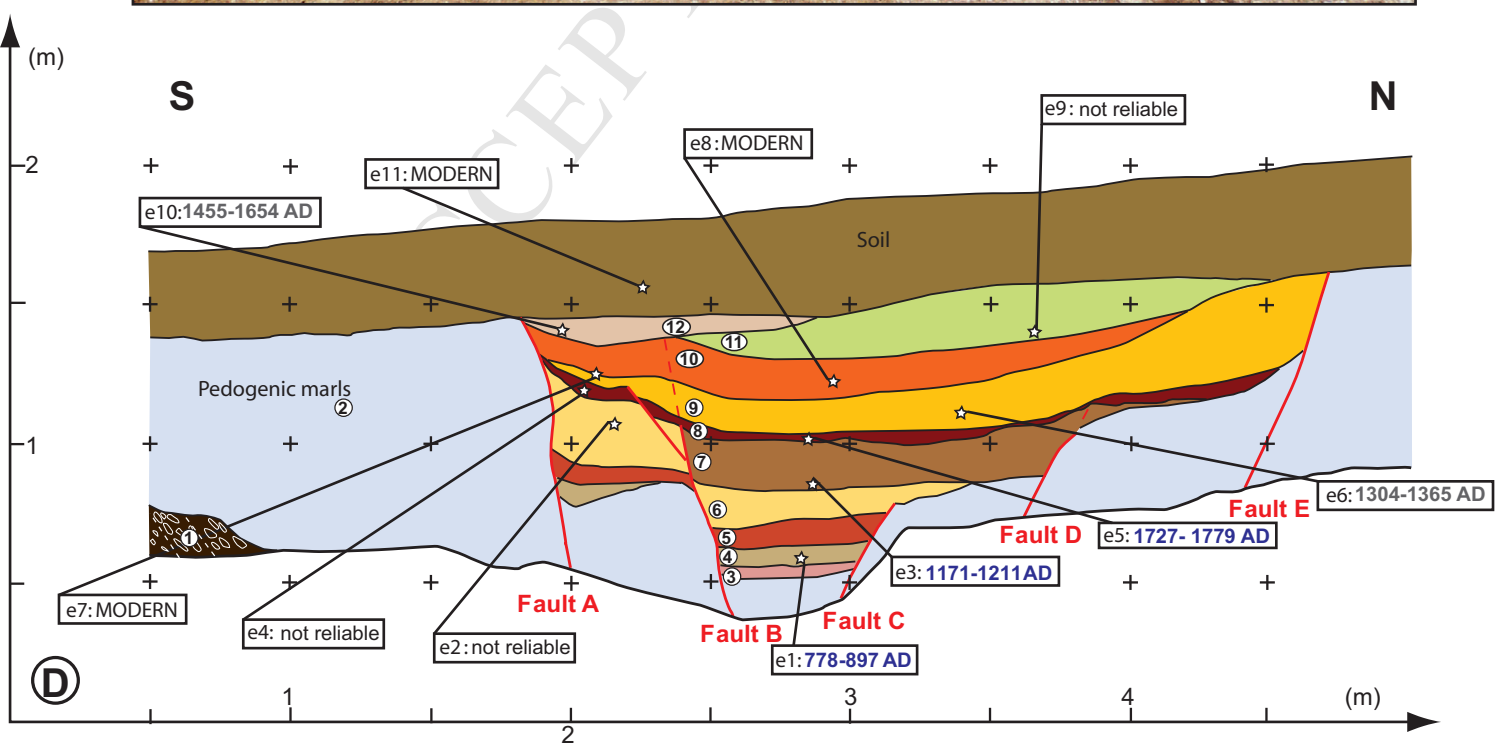
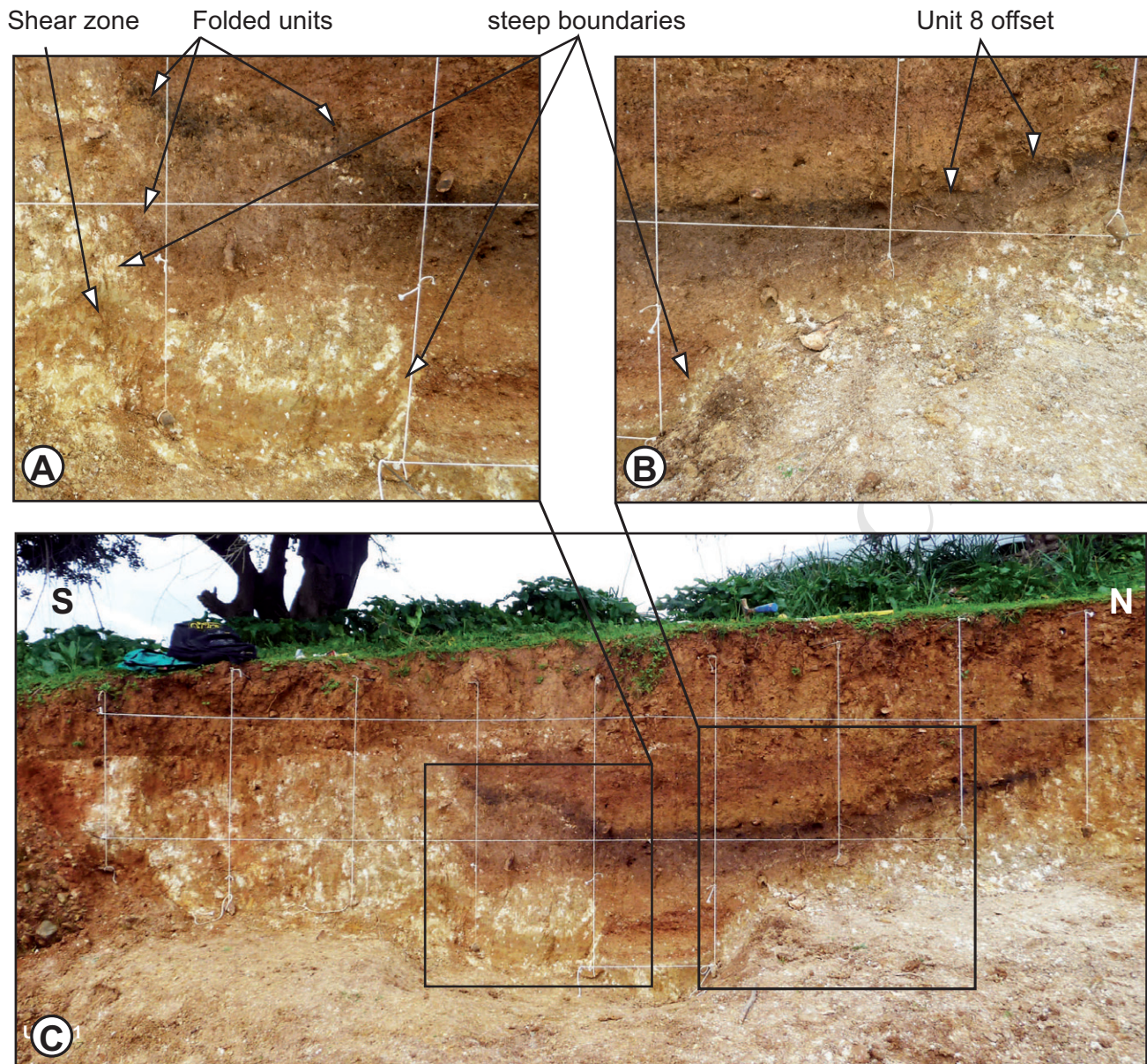


Figure 5

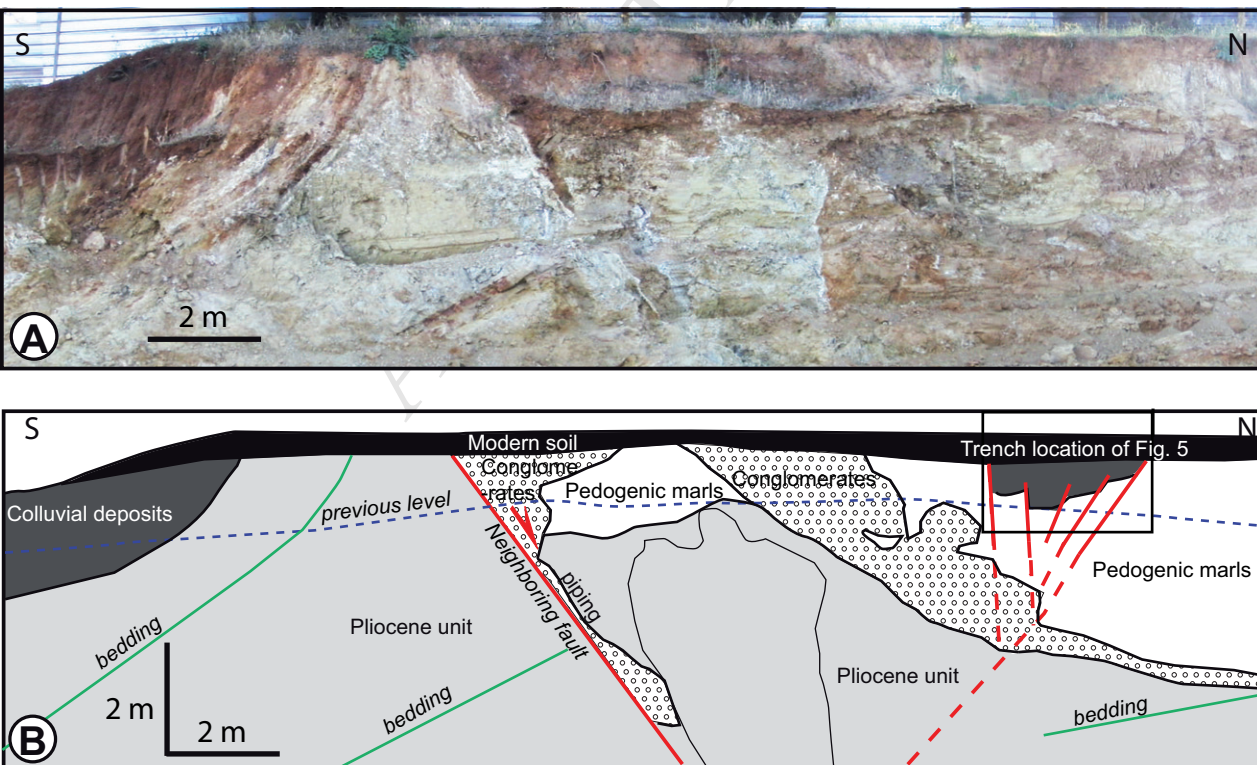


Figure 6

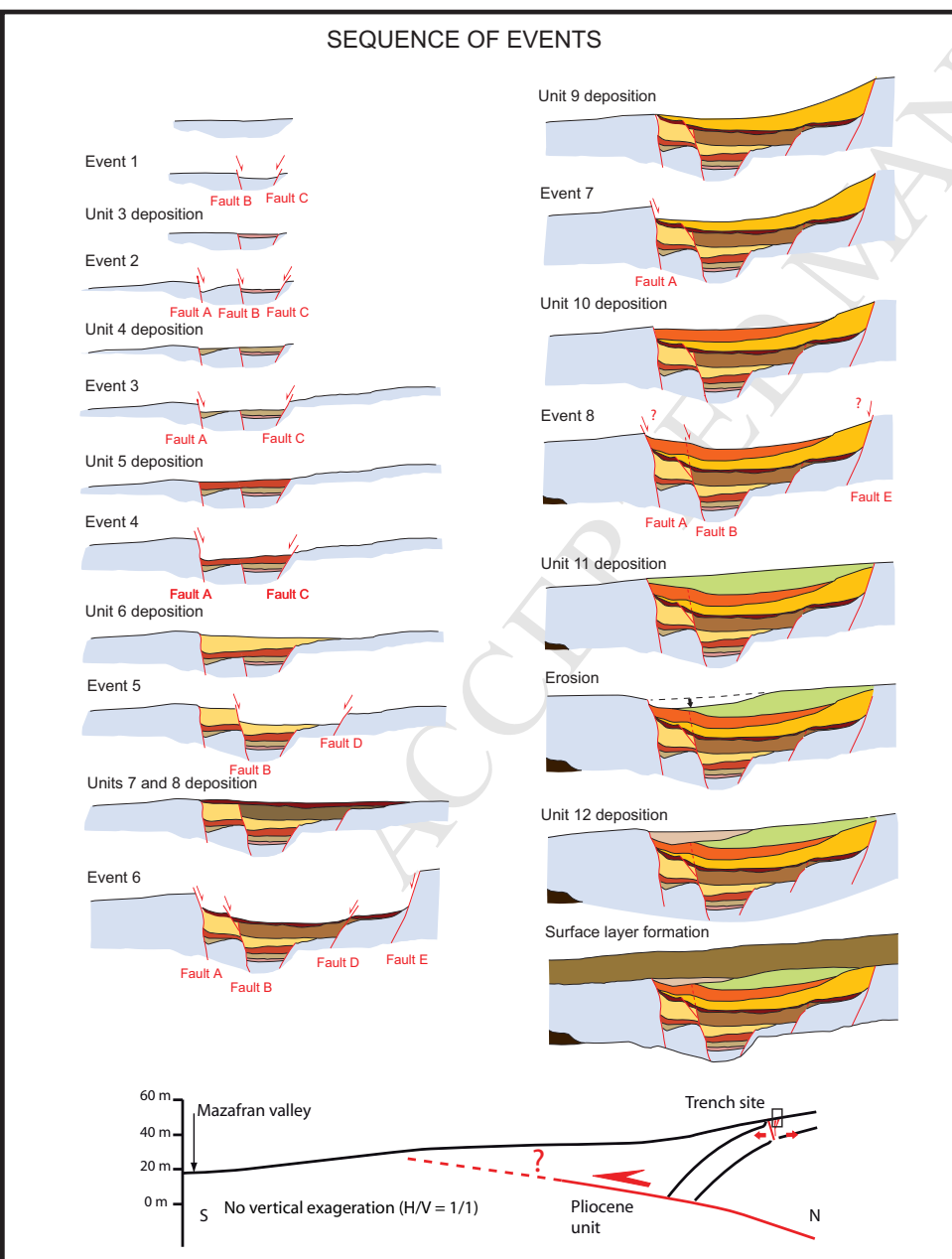


Figure 7

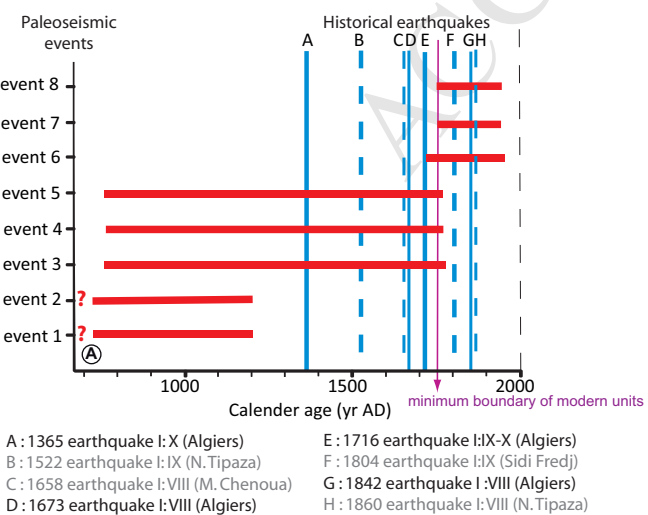
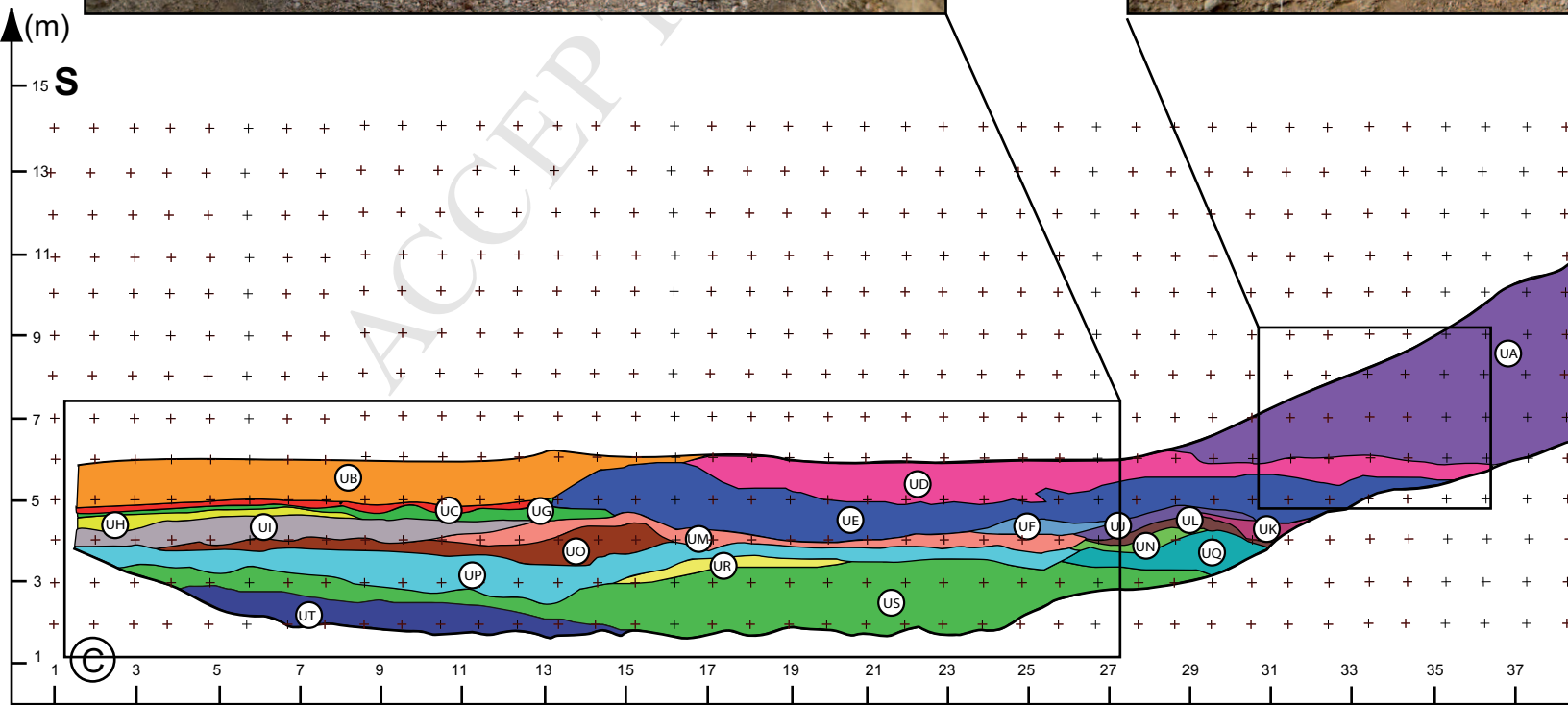


Figure 8



Lithology:

UA: compact brown marl; UB, UC, UD : gravels in ocher clay matrix; UE: gravels in sandy grey matrix; UF: Light grey sand with gravels; UG, UH, UM: cher to yellow clayey silt; UG, UI, UK, UL, UN , UO, UP, UQ: C

Auxiliary material